HEAT AS A PROBE OF SUPERFLUID HELIUM FLOW
PAYNE, RICHARD STEVEN
ProQuest Dissertations and Theses; 1970; ProQuest Dissertations & Theses Global

70-26,195

PAYNE, Richard Steven, 1943-
HEAT AS A PROBE OF SUPERFLUID HELIUM FLOW.

Yale University, Ph.D., 1970
Physics, general

University Microfilms, A XEROX Company, Ann Arbor, Michigan

Copyright by
RICHARD STEVEN PAYNE
1971

THIS DISSERTATION HAS BEEN MICROFILMED EXACTLY AS RECEIVED

Reproduced with permission of the copyright owner. Further reproduction prohibited without permission.

HEAT AS A PROBE OF SUPERFLUID HELIUM FLOW

Richard S. Payne

A Dissertation Presented to the Faculty of the Graduate School of Yale University in Candidacy for the Degree of Doctor of Philosophy 1970.

Reproduced with permission of the copyright owner. Further reproduction prohibited without permission.

Summary

An experiment has been performed to prove that a force exists on a heated body which moves relative to the superfluid component of HeII. We showed that if such a force exists it should modify the logarithmic decrement of a heated, slowly oscillating cylinder in HeII. We measured the decrement of three cylinders as a function of power, as a function of period of oscillation, and as a function of temperature. After a correction, due to a small change in the ordinary viscous damping with heat applied, we compared our data to calculated values of the zero-power decrement and calculated values of the changes in the decrement upon heating. We found that the data agreed very well with our calculations. Since the theoretical calculations involve no adjustable parameters, we could conclude that heat can serve as a probe of the relative velocity of a solid body and the superfluid component of HeII.

Reproduced with permission of the copyright owner. Further reproduction prohibited without permission.

Table of Contents

SECTION I: Introductory Material	1-10
Two Fluid Model	1
Landau Theory and Critical Velocities	6
Persistent Currents	9
SECTION II: Theory	11-30
Review of the Penney Overhausen Theory	11
Oscillating Heated Cylinder	14
Normal Viscous Damping of a Heated Cylinder	20
Summary of Damped Cylinder	29
SECTION III: Experimental Details	31-52
Repetion of Hunt Experiment	31
Apparatus	33
Procedure	43
Possible Sources of Error	46
Data Analysis	48
SECTION IV: Results, Discussion, and Conclusion	53-
Oscillating Experiment Results and Discussion	53
Criticism of the Experiment of Hunt	65
Summary and Conclusions	69

Reproduced with permission of the copyright owner. Further reproduction prohibited without permission.

Appendices 72-89

Appendix I: Torsional Harmonic Oscillator 72

Appendix II: Computer Programs 76

Appendix III: Data 81

References 90

Acknowledgement 93

List of Figures

Figure 1: Tangential velocity near an infinite oscillating plane, heated and unheated. 21

Figure 2: Pumping lines and vibration isolation. 34

Figure 3: Cryostat 35

Figure 4: Cylindrical heaters with geometrical parameters. 37

Figure 5: Heater construction. 38

Figure 6: Cylinder suspension and support. 40

Figure 7: Position detection scheme. 42

Figure 8: Electronics for power application and measurement. 44

Figure 9: Comparison of data to computer fit line. 50

Figure 10: Zero power decrement for Heater #1. 54

Figure 11: $\Delta\delta$ for Heater #1. 55

Reproduced with permission of the copyright owner. Further reproduction prohibited without permission.

Figure 12: Zero power decrement for Heater #2. 57

Figure 13: $\Delta\delta$ for Heater #2. T varied. 58

Figure 14: $\Delta\delta$ for Heater #2. P varied. 59

Figure 15: Zero power decrement for Heater #3. 62

Figure 16: $\Delta\delta$ for Heater #3. T varied. 63

Figure 17: $\Delta\delta$ for Heater #3. P varied. 64

List of Tables

Table 1: Two fluid properties. 1

Table 2: Torque from assymetric heat. 67

Reproduced with permission of the copyright owner. Further reproduction prohibited without permission.

SECTION I

Introductory Material

Two Fluid Model

The two fluid model of HeII was developed independently by Landau[1] on the one hand and Tisza[2] on the other. Landau started from considerations of possible elementary excitations in the liquid, Tisza started from considering liquid heliumas a Bose Einstein gas, but both derived very similar models. They concluded that HeII could be regarded as composed of two mutually interpenetrating components, a superfluid component and a normal fluid component. The following definitional table contains some postulates of the properties of each component.

Postulate I:

Table 1

	density	velocity	specific entropy	viscosity
Normal Fluid Component	ρ_n	v_n	s_n	η
Super-fluid Component	ρ_s	v_s	0	0

Further postulates of the two fluid model are:

Reproduced with permission of the copyright owner. Further reproduction prohibited without permission.

Postulate II: The ordinary density of HeII is

$$\rho = \rho_n + \rho_s$$

Postulate III: The mass current density is

$$\underline{j} = \rho_n \underline{v}_n + \rho_s \underline{v}_s$$

Postulate IV: The superfluid as a whole is a single quantum state described by the order parameter $\psi_s = \sqrt{\rho_s}\, e^{i\phi(\underline{r})}$. Where, ρ_s is the superfluid density and $\phi(\underline{r})$ is the spacially varing phase of the order parameter. This state is the ground state of the total system. It is further supposed that the superfluid density, ρ_s, is a continuous function of temperature between absolute zero and the lambda point, i.e. $\rho_s = \rho_s(T)$. At absolute zero, all of the fluid is in the superfluid state, $\rho_s(0) = \rho$, while at the lambda point, the superfluid density vanishes, $\rho_s(T_\lambda) = 0$.

Postulate V: The normal fluid is in a higher energy state than the superfluid. The energy difference or energy gap between the two states is Ts_n per unit mass.

From these basic postulates we can deduce some of the properties of HeII.

Reproduced with permission of the copyright owner. Further reproduction prohibited without permission.

Deduction I: By substituting the assumed form of the order parameter (Postulate IV) into the quantum mechanical equation of continuity, we can find the form of the superfluid velocity.

$$\psi_s = \sqrt{\rho_s}\, e^{i\phi}$$

$$\rho_s \approx \text{constant}$$

$$\underline{j} = \frac{\hbar}{2mi}\left(\psi_s^* \nabla \psi_s - \psi_s \nabla \psi_s^*\right)$$

$$\underline{j} = \frac{\hbar}{2mi}\left(\rho_s\, i \nabla\phi + \rho_s\, i \nabla\phi\right)$$

$$\underline{j} = \frac{\hbar}{m}\rho_s \nabla\phi$$

$$\therefore \underline{v}_s = \frac{\underline{j}}{\rho_s} = \frac{\hbar}{m}\nabla\phi$$

It then follows that curl $\underline{v}_s = 0$. This condition is commonly referred to as the Landau criterion, because Landau originally postulated it in his theory.

Deduction II: Since the entropy of the total fluid resides solely with the normal fluid, we can write

$$\rho S_{He} = \rho_n S_n$$

Deduction III: Using our Postulates I - IV and the Second Law of Thermodynamics, Tisza[3] was the first to show that the temperature and specific entropy satisfy a wave equation instead of a diffusion equation; implying that

Reproduced with permission of the copyright owner. Further reproduction prohibited without permission.

a much stronger mechanism ("second sound") is available for the propagation of heat in HeII than is available in normal fluids. If a body is heated in HeII, ρ_n is created at the surface, while ρ_s is destroyed. This creates a temporary temperature difference which can be smoothed out by the progagation of ρ_n away from the body and the propagation of ρ_s towards the body. Peshkov[4] was the first to observe "second sound" waves from an oscillating heat source, and he also measured their propagation velocity. Hall[5] later verified that momentum is carried by the two streams of fluid for the case of a steady heat flow.

Deduction IV: Returning to our first deduction, we have shown that $\underline{\text{curl}}\ \underline{v}_s = 0$. Considering a simply connected region of HeII, let us examine an implication of this condition.

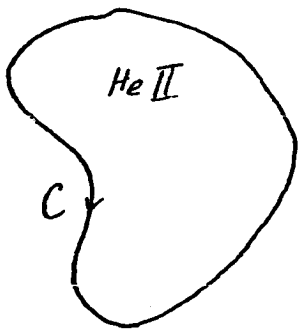

$$\int (\nabla \times \underline{v}_s) \cdot d\underline{S} = 0$$

Invoking Stokes' Theorem

$$\oint_C \underline{v}_s \cdot d\underline{\ell} = 0$$

$$\Gamma \equiv \oint_C \underline{v}_s \cdot d\underline{\ell} = 0$$

Where Γ is the circulation. This means that classical solid body rotation ($\underline{v}_s = \omega r \hat{\theta}$) of a bucket of HeII is impossible for the superfluid component. However,

Reproduced with permission of the copyright owner. Further reproduction prohibited without permission.

Osborne[6] has shown that the superfluid component does participate in the motion when a bucket of HeII is rotated.

Let us suppose that for some reason the superfluid is multiply connected. It is possible to have a circulation with a vanishing curl $\underline{v}_s$ if the circulation is constant around the singularity as shown below.

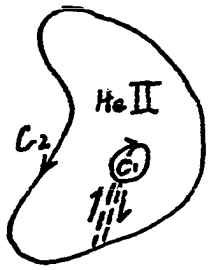

$$\int \nabla \times \underline{v}_s \cdot d\underline{S} = \oint_{C_1+C_2} \underline{v}_s \cdot d\underline{\ell}$$

if $\oint_{C_1} = \Gamma$ and $\oint_{C_2} = -\Gamma$

then $\oint_{C_1} \underline{v}_s \cdot d\underline{\ell} = \Gamma$, while $\nabla \times \underline{v}_s = 0$

We can derive a further condition on the circulation from the fact that $\underline{v}_s = (\hbar/m)\mathrm{grad}(\phi)$.

$$\Gamma = \oint_{C_1} \underline{v}_s \cdot d\underline{\ell}$$

$$\Gamma = \frac{\hbar}{m} \oint_{C_1} \frac{1}{r} \frac{\partial \phi}{\partial \theta} r \, d\theta$$

$$\Gamma = \frac{\hbar}{m} \oint_{C_1} d\phi$$

A single valued wave function requires only that

$$\oint_{C_1} d\phi = 2\pi N \qquad N = 0,1,2,3.....$$

$$\therefore \Gamma = \left(\frac{h}{m}\right) N$$

Reproduced with permission of the copyright owner. Further reproduction prohibited without permission.

Hence, the superfluid circulation is quantized.

Onsager[7] was the first to suggest that quantized vortex lines, the cores of which are devoid of superfluid, might exist in a bath of rotating HeII. The cores of such quantized vortices would render the bath multiply connected, and so allow the circulation which was observed by Osborne. At the same time, the Landau criterion is not violated in the bulk of the fluid, because $\underline{\text{curl}}\ \underline{v}_s = 0$ for a vortex velocity field: $\underline{v}_s = (k/r)\ \hat{\theta}$. Where k is the strength of the vortex line ($k = h/m$) and $\hat{\theta}$ is a unit vector in the θ direction.

Landau Theory and Critical Velocities

Tisza postulated that the superfluid state should have zero viscosity, but Landau reasoned this from his description of possible excitations in the liquid. Landau supposes that the normal component is a gas of quasi-particles (phonons and rotons) occupying the excited states of the system. Phonons are familiar; rotons are elemental vortex motions. The energy of a phonon in terms of its momentum is $E = cp$. Landau postulated that a roton might have an arbitrary energy-

Reproduced with permission of the copyright owner. Further reproduction prohibited without permission.

momentum spectrum, but discarding terms of odd order in the momentum it should be $E = \Delta + p^2/2m^* + 0(p^4)$, where m^* is the effective mass of the roton, and Δ is the energy gap between the lowest phonon and the lowest roton states. Taken together, these two branches of the excited states spectrum should appear as shown below:

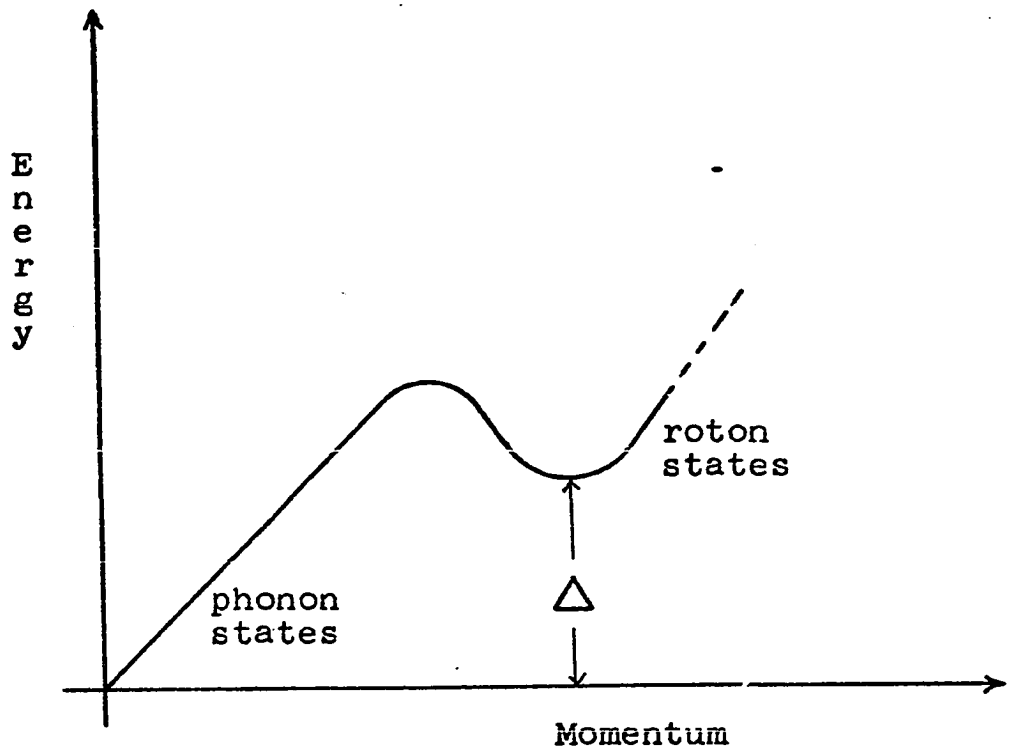

Reproduced with permission of the copyright owner. Further reproduction prohibited without permission.

Landau reasons that the zero viscosity of the superfluid is due to the existence of a nonzero energy gap between the lowest phonon and roton energy states. In order to prevent the superfluid from flowing with zero viscosity it is necessary to give the superfluid sufficient velocity to excite superfluid from the ground state over this gap. Landau calculates how fast the superfluid must move in order to create an excitation. Using current measurements of the excitation spectrum, that critical velocity necessary for the creation of a roton is v_c = 60 m/sec. This number is orders of magnitude larger than any critical velocities which have been observed.[8] It is clear that mechanisms other than the creation of elementary excitations cause the breakdown of superfluidity. Feynman[9] was the first to show that quantized vortex lines are one such possible mechanism. He showed that smaller velocities of flow, dependant on the size of the container, are sufficient to provide the energy necessary for the creation of vortex rings (a vortex ring is a line closed upon itself).

The two fluid model with the inclusion of quantized vortices is sufficient to describe all of the effects which we have observed, and we shall use this model to discuss our work.

Reproduced with permission of the copyright owner. Further reproduction prohibited without permission.

Persistent Currents

We have shown that the superfluid circulation in a multiply connected region is quantized, and that for dissipation to occur in the flow of superfluid it must flow sufficiently fast. It then seems obvious, as it did to many investigators, that should a circulation be established in a multiply connected region of a magnitude such that no critical velocity were exceeded, this circulation should persist. Andronikashvili[10] first attempted to observe superfluid persistent currents, but his experiment failed. However, other experiments have now verified the existence of persistent currents. One such experiment by Reppy and Depatie[11] has important bearing on what follows and we shall briefly discuss it at this point.

They took a bucket packed with a closely spaced stack of disks, filled it with liquid helium, and suspended it from a virtually frictionless bearing. Maintaining the temperature $T < T_\lambda$, they rotated the bucket faster than a critical frequency ω_c, and then decelerated the bucket slowly to rest. After a waiting period, long enough to allow the normal fluid motion to decay, they pulsed the bucket with an impulse of heat.

Reproduced with permission of the copyright owner. Further reproduction prohibited without permission.

They observed that the bucket accelerated, and from the magnitude of the acceleration they were able to measure the angular momentum stored in the superfluid persistent current, which they found to be proportional to $\omega_c \rho_s(T)$. Furthermore, they found that if the temperature of the bucket was slowly changed to another temperature T' while the bucket was held at rest (before the heat pulse), and then the bucket was heated with a large heat pulse, the angular momentum of the persistent current was proportional to $\omega_c \rho_s(T')$. This experiment and its precise refinement by Clow and Reppy[12] clearly show that if the superfluid state has a velocity field $\underline{v}_s(\underline{r})$, and the temperature is reduced slowly, the new ρ_s which condenses into the superfluid state must also have that velocity field. This is consistent with the picture that the superfluid consists of a <u>single</u> quantum state which is macroscopically occupied. The existence of this unique superfluid flow state is important to arguments which we shall present.

Reproduced with permission of the copyright owner. Further reproduction prohibited without permission.

SECTION II

Theory

Review of the Penney Overhauser Theory

Penney and Overhauser[13] (hereafter designated PO) have recently predicted that a new tool may be available for the study of superfluid flows. They predicted that there should exist a torque γ on a heated cylinder about which there is a superfluid circulation Γ and that it should be given by:

$$\gamma = \frac{\Gamma \dot{Q}}{2\pi s_n T} \qquad (1)$$

where T is the Kelvin temperature and $\dot{Q}$ is the total power dissipated at the surface of the heater.

We can understand the source of this torque as follows. If a total power $\dot{Q}$ is applied to the surface of a cylinder, superfluid is destroyed at a rate $\dot{M}_s = -\dot{Q}/Ts_n$. This superfluid is converted at the same rate into normal fluid, which must interact with the surface. If the superfluid is flowing with a velocity, v_s at a radius "a" when converted to normal fluid, it will transfer angular momentum to the heater at a rate

Reproduced with permission of the copyright owner. Further reproduction prohibited without permission.

$$\dot{L} = \left(\frac{\dot{Q}}{T s_n}\right) v_s a \qquad (2)$$

We know that the superfluid circulation is

$$\Gamma = \oint \underline{v}_s \cdot d\underline{l} = 2\pi a v_s \qquad (3)$$

Substituting for (av_s) from equation (3) into equation (2), we have the result of PO:

$$\dot{\gamma} = \frac{\Gamma \dot{Q}}{2\pi s_n T}$$

Hence, the torque, which they predicted, is caused by the transfer of momentum from the superfluid flow to the heated surface by the destruction of superfluid.

One aspect of this torque which should be noticed is that it is a steady torque rather than a ballistic torque. The superfluid state is one unique ground state. The velocity of the superfluid is determined by the phase of the wave function of the ground state. If the temperature is held constant during the heating of the cylinder, while normal fluid is created at the surface of the heater, superfluid is created at the

Reproduced with permission of the copyright owner. Further reproduction prohibited without permission.

source of refrigeration needed to maintain the temperature constant. Since the superfluid state is unique, the new superfluid created at the refrigeration site must fall in step with the existing superfluid. This means that as long as no critical velocity is exceeded the velocity of the superfluid at the surface of the heater will remain the same and so the torque will also remain the same.

The experiment of Reppy and Depatie discussed in the previous section provides evidence that the superfluid velocity field is indeed preserved. In their experiment, they cooled a superfluid "persistent current" and saw an increase in the angular momentum of that current. In the case of the torque proposed by PO, superfluid is both destroyed and created, but the velocity field is also preserved.

Reproduced with permission of the copyright owner. Further reproduction prohibited without permission.

Oscillating Heated Cylinder

A case very similar to the one discussed, and the case of primary interest to the author is that of a heated cylinder oscillating in HeII. It is well known[14] that ρ_s is not excited into motion by an oscillating cylinder provided the amplitude of oscillation is not too large and its period not too short. If an oscillating cylinder is heated, a drag will be caused by the creation of stationary ρ_n, at the surface of the heater, which must be accelerated to the velocity of the surface.

If a cylinder is suspended from a torsion fiber and allowed to oscillate freely, it will undergo damped harmonic motion. The angular displacement as a function of time will be given by:

$$\theta = \theta_0 e^{-\frac{\delta t}{P}} \cos(\omega t + \phi)$$

where ω is the angular frequency, "P" is the period, and δ is the logarithmic decrement. The amplitude θ_0 and the phase ϕ are both determined by the initial conditions. The decrement can be measured accurately and the drag caused by the PO force should produce an

Reproduced with permission of the copyright owner. Further reproduction prohibited without permission.

easily detectable change in the decrement.

In order to calculate the effect of the PO torque on the logarithmic decrement, we shall assume that the change in the decrement due to the PO torque, $\Delta\delta_{PO}$, is much less than unity, and also that the logarithmic decrement from all other sources in much less than unity. With these assumptions, all contributions to the decrement can be calculated separately from the work done by a given force over a cycle of oscillation. The decrement is equal to the energy loss per cycle divided by twice the energy stored in the oscillator.[15] We have derived these properties of the harmonic oscillator in Appendix I.

Starting from the result of PO,

$$\chi = \frac{\Gamma \dot{Q}}{2\pi s_n T}$$

we notice that if the superfluid is stationary, and the cylinder is moving with an angular velocity $\dot{\theta}$, the heater sees an equivalent circulation

$$\Gamma = \oint \underline{v} \cdot d\underline{\ell}$$

Reproduced with permission of the copyright owner. Further reproduction prohibited without permission.

$$\Gamma = \int_0^{2\pi} a^2 \dot{\theta}\, d\phi$$

$$\Gamma = 2\pi a^2 \dot{\theta}$$

Hence, for the oscillating case there should also be a torque

$$\tau = \frac{a^2 \dot{Q}}{S_n T}\, \dot{\theta} \equiv c\dot{\theta}$$

If we assume

$$\theta = \theta_0 \cos(\Omega t)$$

then

$$\dot{\theta} = -\Omega \theta_0 \sin(\Omega t)$$

Calculating the work done over one cycle by the PO torque

$$\Delta E_{PO} = \oint_{cycle} \tau\, d\theta$$

$$\Delta E_{PO} = \oint_{cycle} c\dot{\theta}\, d\theta$$

Reproduced with permission of the copyright owner. Further reproduction prohibited without permission.

With the substitution $\phi = \Omega t$ we have

$$\Delta E_{PO} = \int_0^{2\pi} c\,\theta_0^2\,\Omega \sin^2\phi \, d\phi$$

$$\Delta E_{PO} = \pi c \theta_0^2 \Omega$$

The total energy stored in a torsional pendulum is

$$E_0 = \frac{1}{2} I \Omega^2 \theta_0^2$$

Remembering that the change in the decrement is equal to the energy loss per cycle divided by twice the energy stored, we have

$$\Delta\delta_{PO} = \frac{\Delta E_{PO}}{2E_0}$$

$$\Delta\delta_{PO} = \frac{\pi c}{I\Omega}$$

$$\Delta\delta_{PO} = \frac{Pc}{2I}$$

Substituting for $c = a^2\dot{Q}/s_n T$ in this expression we finally have an expression for the change in the decrement from the PO torque:

$$\Delta\delta_{PO} = \frac{Pa^2\dot{Q}}{2I s_n T}$$

Reproduced with permission of the copyright owner. Further reproduction prohibited without permission.

We have assumed that $\Delta\delta_{PO}$ is much less than unity. We can insert numbers into the above expression to verify that assumption.

$P = 20$ sec

$a = .75$ cm

$I = 1$ gm-cm^2

$T = 2$ K

$s_n = 1.72 \times 10^3$ mw-sec/K

$\dot{Q} = 10$ mw

Then $\Delta\delta_{PO} \approx 1.7 \times 10^{-2} \ll 1$. From our experimental measurements, we know also that $\delta \leq 10^{-1}$.

The purpose of this theoretical introduction is to develop expressions for theoretical predictions which we shall compare to experiments later in the text, but a small digression is here needed to provide motivation for the following discussion. Experiments were performed which measured the change in the decrement versus power for an oscillating cylinder, and these results were compared to the expression derived from the PO force. The change in the damping with power did not agree with the calculations and it was suggested[16] that the normal viscous forces might be modified by the flow of ρ_n induced by the application of heat. Then, subsequent

Reproduced with permission of the copyright owner. Further reproduction prohibited without permission.

to the experiment, we performed the following calculation which shows indeed that the normal fluid viscous forces are modified by the radial flow of the normal fluid in our experiment. It is only for the sake of organization that we present the calculation first in this thesis.

Reproduced with permission of the copyright owner. Further reproduction prohibited without permission.

Normal Viscous Damping of a Heated Oscillating Cylinder

The oscillating disk in HeII has been the object of many studies. It has been used to determine the viscosity,[17,18,19,20,21] the normal fluid density ρ_n,[18,20,21] and the superfluid critical velocity.[18] As a result, the hydrodynamic equations for the system have often been examined, but we find it necessary to again examine the problem with the inclusion of heated surfaces. As we shall show, the application of heat modifies the drag of the normal fluid viscosity. In this section we hope to give a physical picture of the mechanism for this modification, and then derive a more accurate result.

For simplicity, consider the case of an infinite y-z plane executing sinusoidal oscillations parallel to the y axis. The solution for the normal fluid velocity field, v_{ny}, can be found in most elementary books on hydrodynamics;[22] it is an exponentially damped plane wave as sketched in Figure 1a. If no heat is applied, the other components of the velocity, v_{nx} and v_{nz}, will be zero. When uniform heat is applied to the surface of the plane, ρ_n will stream away from the surface and ρ_s will stream towards the surface to take

Reproduced with permission of the copyright owner. Further reproduction prohibited without permission.

Figure 1

Figure 1 a .

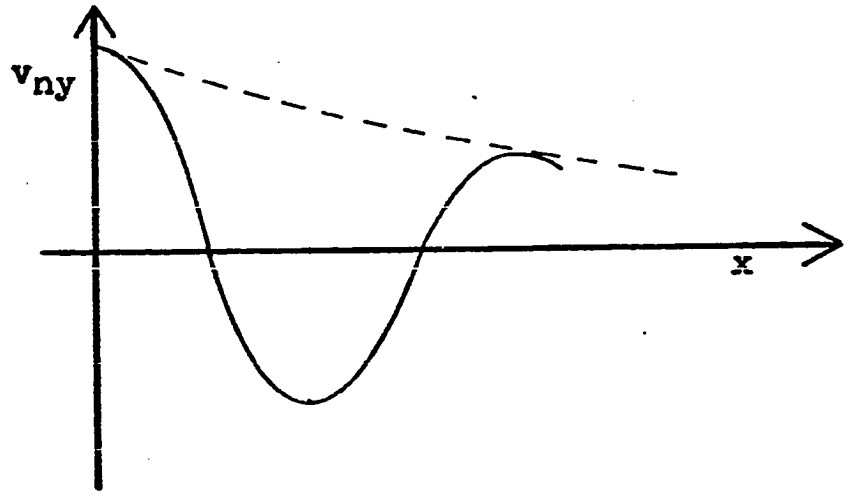

The tangential velocity field of an infinite oscillating plane with no heat flow.

Figure 1 b .

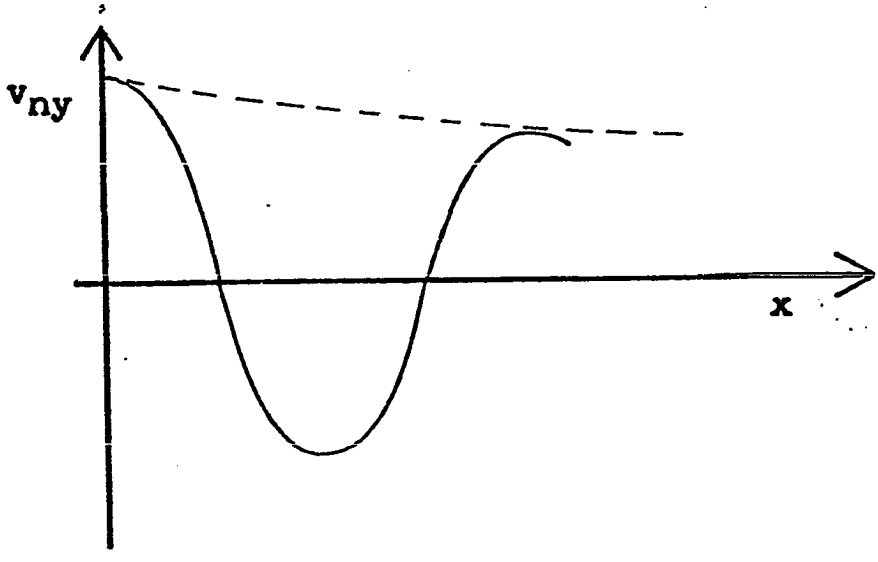

The tangential velocity field of an infinite oscillating plane with heat flow.

Reproduced with permission of the copyright owner. Further reproduction prohibited without permission.

its place. This means that there will be an x component of the normal fluid velocity as well. The inclusion of this component into the hydrodynamic equations causes a modification of the envelope of the viscous waves. Physically the viscous wave is "blown away" from the surface by the heat induced motion in the x direction. The velocity field v_{ny}, with heat will appear as shown in Figure 1b.

The viscous drag per unit area on the y-z plane is proportional to the gradient of the normal fluid velocity at the surface. One can easily see that the gradient will be smaller for the less steeply damped viscous wave of Figure 1b than for the unheated viscous waves. If one applies these arguements to a freely oscillating cylinder, a smaller drag force means a smaller logarithmic decrement, hence, the application of heat should decrease the normal viscous contribution to the decrement in competition with the effect of the PO force which tends to increase the decrement.

To solve for the viscous contribution to the logarithmic decrement of a heated cylinder, we shall proceed in the same manner as we did for the PO contribution. We shall find the viscous forces on the cylinder, assume

Reproduced with permission of the copyright owner. Further reproduction prohibited without permission.

the decrement is small, and, from the work done by the viscous forces, calculate the decrement. In order to find the viscous force, we must first solve the Navier Stokes equation for the tangential velocity field of the normal fluid. With this solution we can examine the momentum stress tensor to find the force. We shall solve for the velocity field near an infinitely long cylinder, and assume that the solution is valid for our cylinders of finite length. We believe that this assumption is valid because the penetration depth of viscous waves is at most 2mm, and generally much less than 1mm. Since the lengths of the cylinders which we used were from 6 to 30 mm, they are long compared to the dimension over which we would expect changes in the solutions.

Starting from the Navier Stokes equation for the cylindrical component of the velocity field:

$$\frac{\partial v_\phi}{\partial t} + v_r \frac{\partial v_\phi}{\partial r} + \frac{v_\phi}{r}\frac{\partial v_\phi}{\partial \phi} + v_z \frac{\partial v_\phi}{\partial z} + \frac{v_r v_\phi}{r} =$$

$$\frac{1}{\rho r}\frac{\partial \psi}{\partial \phi} + \nu\left(\frac{\partial^2 v_\phi}{\partial r^2} + \frac{1}{r^2}\frac{\partial^2 v_\phi}{\partial \phi^2} + \frac{\partial^2 v_\phi}{\partial z^2} + \frac{1}{r}\frac{\partial v_\phi}{\partial r} + \frac{2}{r^2}\frac{\partial v_r}{\partial \phi} - \frac{v_\phi}{r^2}\right)$$

where v_n, v_ϕ, and v_z refer to the normal fluid velocity. "ψ" is the pressure.

Reproduced with permission of the copyright owner. Further reproduction prohibited without permission.

We shall assume:

1. $v_\phi(r,t) = v_\phi(r)e^{-i\omega t}$,
2. A uniform heat per unit area, $\dot{q}$, is applied at the surface of the cylinder.

The radial velocity of fluid near a torsionally oscillating cylinder will normally be zero, however, with heat applied, the velocity will be $v_r = v_n a/r$, where $v_n = \dot{q}/\rho sT$.

Substituting the time dependance from assumption 1 and the radial component of the velocity field derived from assumption 2, and discarding all ϕ and z derivatives as zero from the symmetry of the problem, we are left with the simpler differential equation:

$$-i\omega v_\phi + \frac{v_n a}{r} v_\phi' + \frac{v_n a}{r^2} v_\phi = \nu\left(v_\phi'' + \frac{1}{r} v_\phi' - \frac{v_\phi}{r^2}\right)$$

where primes denote differentiation with respect to "r". Reorganizing this equation we can recognize it as one whose solution is a Bessel function.[28]

$$v_\phi'' + \frac{\left(1 - \frac{v_n a}{\nu}\right)}{r} v_\phi' + \left(\frac{i\omega}{\nu} - \frac{\left(1 + \frac{v_n a}{\nu}\right)}{r^2}\right) v_\phi = 0$$

The solution is:

$$v_\phi = c\, r^\alpha Z_{1+\alpha}(\beta r)$$

Reproduced with permission of the copyright owner. Further reproduction prohibited without permission.

Where $Z_{1+\alpha}$ is a Bessel function of order $1+\alpha$, $\alpha = v_n a/2\nu$, $\beta = (1+i)/\lambda$, λ is the penetration depth of viscous waves, $\lambda = (\omega/2\nu)^{1/2}$, $i = (-1)^{1/2}$, and ν is the kinematic viscosity.

Under the boundary conditions:

1. $v_\phi = 0$ at $r = \infty$,
2. $v_\phi = u_o e^{-i\omega t}$ at $r = a$,

we can determine the constant "c" and the type of Bessel function. Boundary condition 1 forces us to chose the Hankel function of the first kind, and the second condition allows us to determine

$$c = \frac{u_o e^{-i\omega t}}{a^\alpha H^{(1)}_{1+\alpha}(\beta a)}$$

We can now calculate the force per unit area from the ϕ,r component of the momentum stress tensor (dot product of momentum stress tensor with $\hat{n}$):[23]

$$F_A = \eta\left(\frac{1}{r}\frac{\partial v_r}{\partial \phi} + \frac{\partial v_\phi}{\partial r} - \frac{v_\phi}{r}\right)\Big|_{r=a}$$

From symmetry we know that $\frac{\partial v_r}{\partial \phi} = 0$.

Inserting our solution for the velocity we have:

Reproduced with permission of the copyright owner. Further reproduction prohibited without permission.

$$F_A = \eta \left(\frac{\partial}{\partial r} \left(c r^{\alpha} H_{1+\alpha}^{(1)}(\beta r) \right) \Big|_{r=a} - c a^{\alpha-1} H_{1+\alpha}^{(1)}(\beta a) \right.$$

making use of the differential formula for the Bessel functions[24]

$$\frac{\partial H_{1+\alpha}^{(1)}(\beta r)}{\partial r} = \beta \left(\frac{-(1+\alpha)}{\beta a} H_{1+\alpha}^{(1)}(\beta a) + H_{\alpha}^{(1)}(\beta a) \right)$$

we find

$$F_A = \eta \left(-2c a^{\alpha-1} H_{1+\alpha}^{(1)}(\beta a) + c\beta a^{\alpha} H_{\alpha}^{(1)}(\beta a) \right)$$

and finally

$$F_A = \eta u_0 e^{-i\omega t} \left(-\frac{2}{a} + \beta \frac{H_{\alpha}^{(1)}(\beta a)}{H_{1+\alpha}^{(1)}(\beta a)} \right)$$

Applying this solution to a finite section of cylindrical wall of height "h", we have

$$F = 2\pi a h \eta u_0 e^{-i\omega t} \left(-\frac{2}{a} + \beta \frac{H_{\alpha}^{(1)}(\beta a)}{H_{1+\alpha}^{(1)}(\beta a)} \right)$$

Landau and Lifshitz[25] show that the rate of loss of

Reproduced with permission of the copyright owner. Further reproduction prohibited without permission.

energy loss from such a complex force is

$$\dot{\bar{E}} = \frac{1}{2} \mathrm{Re}\left\{ \frac{F}{u_0 e^{-i\omega t}} \right\} |u_0|^2$$

Substituting for $|u_0|^2 = \theta_0^2 \omega^2 a^2$, our solution for the force, and multiplying the energy loss rate by the period, we find the energy loss per cycle

$$\Delta E = 2\pi^2 a^3 h \eta \theta_0^2 \omega \left(-\frac{2}{a} + \mathrm{Re}\left\{ \beta \frac{H_\alpha^{(1)}(\beta a)}{H_{1+\alpha}^{(1)}(\beta a)} \right\} \right)$$

The total energy stored in the torsional oscillations is

$$E_0 = \frac{1}{2} I \omega^2 \theta_0^2$$

Finally, we have the contribution to the decrement from the heated section of the cylinder is

$$\delta_{vh} = \frac{\Delta E}{2 E_0}$$

$$\delta_{vh} = \frac{2\pi^2 a^3 h \eta}{I \omega} \left(-\frac{2}{a} + \mathrm{Re}\left\{ \beta \frac{H_\alpha^{(1)}(\beta a)}{H_{1+\alpha}^{(1)}(\beta a)} \right\} \right)$$

Subtracting the zero power decrement for the same section of cylinder, we have an expression for the change in the damping with power:

Reproduced with permission of the copyright owner. Further reproduction prohibited without permission.

$$\Delta\delta_{vh} = \frac{2\pi^2 a^3 h \eta}{I\omega}\left(Re\left\{\beta\frac{H_0^{(1)}(\beta a)}{H_1^{(1)}(\beta a)}\right\} - Re\left\{\beta\frac{H_\alpha^{(1)}(\beta a)}{H_{1+\alpha}^{(1)}(\beta a)}\right\}\right)$$

Finally we need an expression for the contributions of the top of the cylinder and for the unheated length of wall which we shall call "L". This problem has been solved by Dash and Taylor[20] to greater precision than we have required for this study. Using their results, but discarding terms for corner corrections and second order terms we have

$$\delta_{vuh} = \frac{\pi^2 a^4 \eta}{\lambda\omega I}\left(1 + \frac{2L}{a} + \frac{3\lambda L}{a^2}\right)$$

for the contribution to the decrement from unheated portions of the cylinder.

Reproduced with permission of the copyright owner. Further reproduction prohibited without permission.

Summary of the Damped Cylinder

Most of the results which we shall discuss are results of the damping of heated oscillating cylinders. We shall be concerned mainly with the changes which occur upon heating, but we shall also calculate the zero power damping and compare it to the experiment because it confirms our assumption that the flow around the cylinder is laminar viscous flow.

The zero power damping should be composed of two parts. There will be one contribution from the suspension which we can measure by observing the damping of the pendulum in a high vacuum; call this contribution δ_{Vac}. There will be another contribution from the effects of the viscous normal fluid. The second part we will subdivide into two parts again; the first part, δ_{Vh}, is the viscous contribution of the section of the cylinder to be heated, and the second part, δ_{Vuh}, is the viscous contribution of the rest of the cylinder. As we have shown, if a section of the side wall of the cylinder of length "h" is heated, and a section of length "L" is unheated, the zero power damping is given by:

Reproduced with permission of the copyright owner. Further reproduction prohibited without permission.

$$\delta_0 = \delta_{Vac} + \delta_{Vh} + \delta_{Vah}$$

$$\delta_0 = \delta_{Vac} + \frac{2\pi^2 a^3 h \rho}{I\omega}\left(-\frac{2}{a} + Re\left\{\beta\frac{H_0^{(1)}(\beta a)}{H_1^{(1)}(\beta a)}\right\}\right) + \frac{\pi^2 a^4 \rho}{\lambda\omega I}\left(1 + \frac{2L}{a} + \frac{3\lambda L}{a^2}\right)$$

The change in the decrement will be the sum of the change due to the PO effect, $\Delta\delta_{PO}$, plus the change in the viscous damping from heat, $\Delta\delta_{Vh}$, which we have already separately derived. For convenience we present their sum:

$$\Delta\delta = \Delta\delta_{PO} + \Delta\delta_{Vh}$$

$$\Delta\delta = \frac{Pa^2 Q}{2I S_n T} + \frac{2\pi^2 a^3 h \rho}{I\omega}\left(Re\left\{\beta\frac{H_0^{(1)}(\beta a)}{H_1^{(1)}(\beta a)}\right\} - Re\left\{\beta\frac{H_\alpha^{(1)}(\beta a)}{H_{1+\alpha}^{(1)}(\beta a)}\right\}\right)$$

Our results will be presented in comparison with these formulas.

Reproduced with permission of the copyright owner. Further reproduction prohibited without permission.

SECTION III

Experimental Details

Repetition of Hunt Experiment

The experiment as originally conceived envisioned a repetition of Hunt's [26] experiment with the use, however, of improved techniques based upon a considerable body of experience with rotating helium evolved over the years by our group.

We isolated the helium under investigation from the main bath, we restricted the geometry to provide higher critical velocities and hence larger circulations, we devised a multiply connected geometry, and we heated the cylinder electrically. We performed many runs using many procedures, but we did not observe torques which we could unambiguously prove were associated with the PO effect. On occasion, we did see torques which were probably due to the effect, but these were always superimposed on spurious torques. We could not be certain whether the failure of the experiment was due to our inability to create reproducable persistent currents, or due to the failure of the PO prediction. Since the spurious torques which we saw were often much larger

Reproduced with permission of the copyright owner. Further reproduction prohibited without permission.

than the torques which Hunt had taken as proof of the PO prediction, we began to seriously doubt the conclusions of his work, and we felt that a more rigorous proof of the PO predictions was worthwhile. As we have explained in the previous sections, the change in the decrement of a heated oscillating cylinder provides an excellent means of observing the effects of the PO force where all the variables of the experiment are known. The circulation, unknown in the Hunt experiment, is determined by the motion of the cylinder in our version of the experiment. We need only assume that the superfluid remains at rest, a very reasonable assumption.

The rest of this section consists of a description of the experimental details of the measurements of the logarithmic decrement.

Reproduced with permission of the copyright owner. Further reproduction prohibited without permission.

Apparatus

The apparatus which we used for the measurement of the logarithmic decrement is shown in Figures 2 to 7.

Figure 2 shows the valving which we used to control the temperature of the helium bath, as well as the vibration isolation needed to isolate the experiment from the vibrations of the main pumping line and those which are caused by opening and closing the various valves of the pumping station. Each of the main vacuum lines was connected to a Kinney KT 150 high capacity mechanical vacuum pump. The 30" section of 1" I.D. rubber hose, which we inserted in the line for vibration isolation, limited the pumping speed of our pumping station so that the minimum attainable temperature was 1.25 K.

The next view, Figure 3, shows a closer view of the cryostat. The oscillating cylinder was positioned at the bottom of a 5" I.D. helium dewar flask. With the addition of a "Kimwipe" baffle, the running time between fills of the dewar was more than two days. Hence, we were able to fill the helium dewar once, and then take all the measurements of the logarithmic decrement which we desired without the necessity of disturbing the

Reproduced with permission of the copyright owner. Further reproduction prohibited without permission.

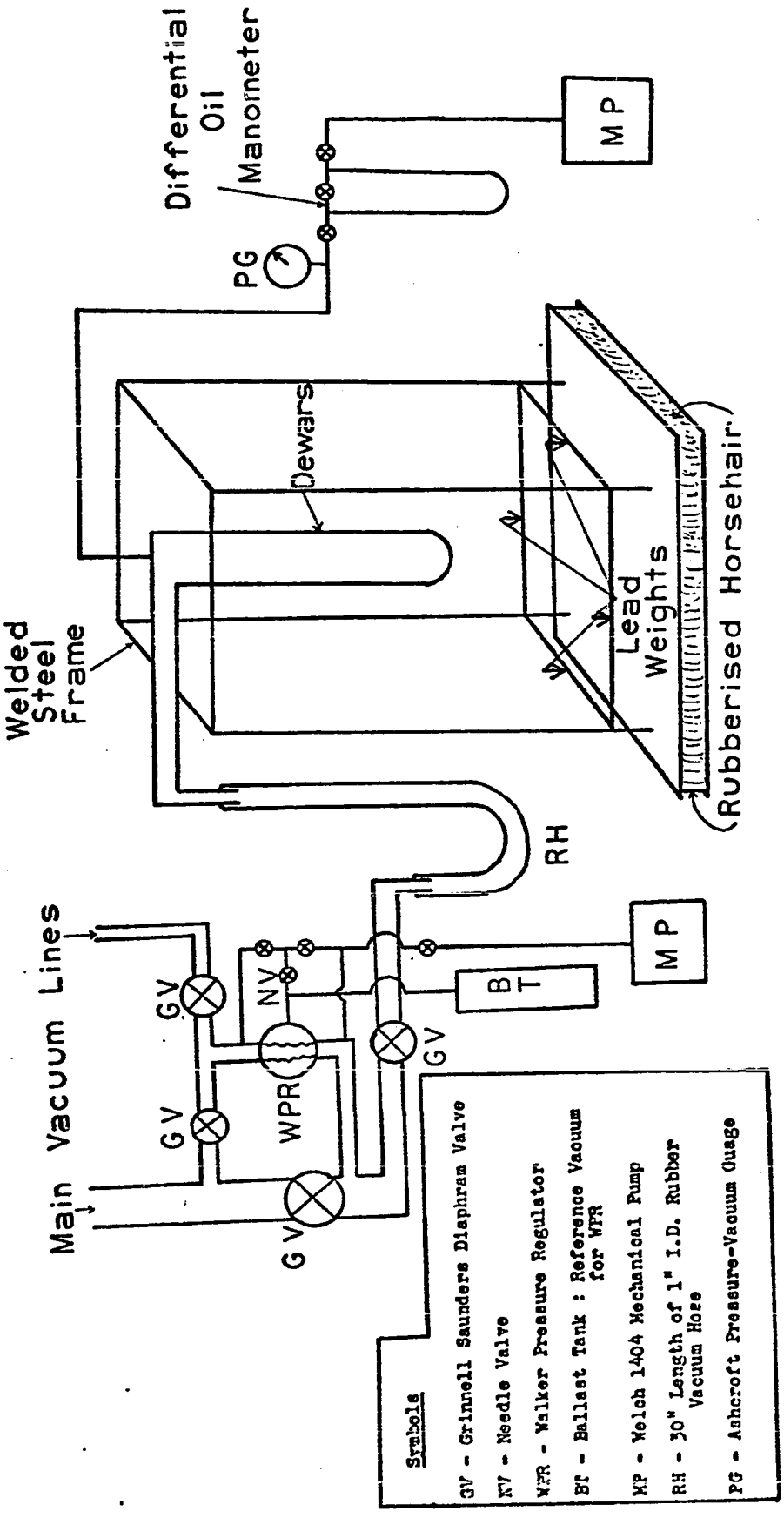

Figure 2. PUMPING LINES & VIBRATION ISOLATION

Reproduced with permission of the copyright owner. Further reproduction prohibited without permission.

Figure 3

Cryostat

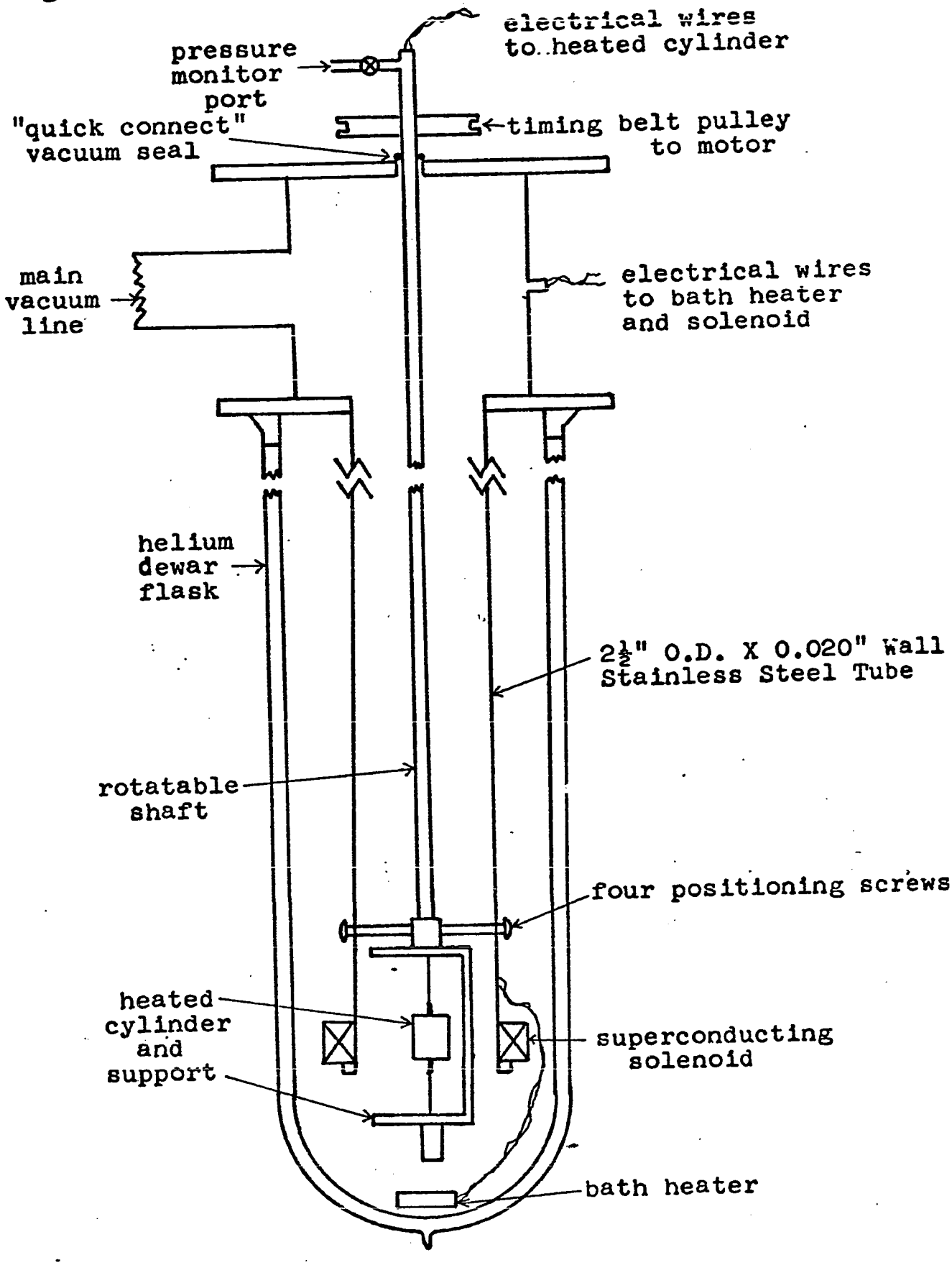

Reproduced with permission of the copyright owner. Further reproduction prohibited without permission.

heater and suspension with an additional transfer of helium.

Three different heaters were used for measurements of the heated logarithmic decrement. The three heaters, #1, #2, and #3, are shown in Figure 4. Number 1, as shown in Figure 5, is a composition of phenolic and magnesium onto which was painted a film of Aqua-Dag, a colloidalsolution of graphite in water. The graphite provided a resistive coating which could be heated electrically. Silver paint was used to make the necessary electrical bridges on the heater. The other heaters, were made from hollow glass bulbs coated with a film of Nichrome. Nichrome was chosen for its high resistivity. The bulbs were rotated during the coating process to insure uniform coatings of Nichrome. As is shown in Figure 5, the coating was done in two steps, using movable baffles, so that a thin, high resistance, film of Nichrome was deposited along the straight cylindrical wall, and a thicker, low resistance, film was deposited over the rest of the bulb. The Nichrome was evaporated onto heater #2, sputtered onto heater #3. Silver paint was again used to make contact from the thick Nichrome films to the collar which anchored

Reproduced with permission of the copyright owner. Further reproduction prohibited without permission.

Figure 4

Cylindrical Heaters with Geometrical Parameters

Composition Heater

#1

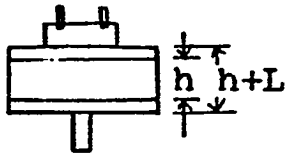

I = 0.965 g-cm^2
a = 0.851 cm
h+L = 0.80 cm
h = 0.40 cm
A = 2.14 cm^2

#2

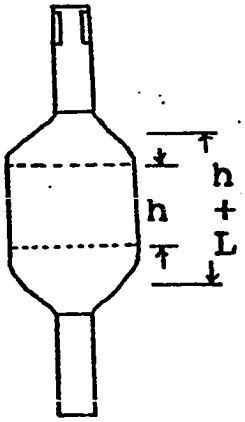

I = 0.999 g-cm^2
a = 0.756 cm
h+L = 1.6 cm
h = 0.90 cm
A = 4.3 cm^2

Nichrome Glass Bulb Heaters

#3

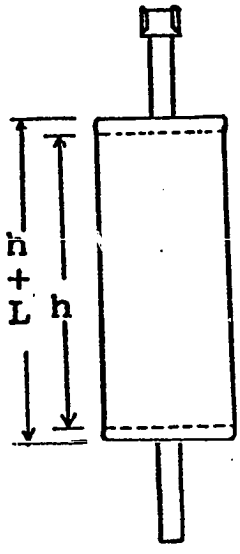

I = 0.969 g-cm^2
a = 0.724 cm
h+L = 3.8 cm
h = 3.4 cm
A = 15.4 cm^2

I = moment of inertia, a = radius, h + L = total length of cylinder, h = length of heated section, A = heated area.

Reproduced with permission of the copyright owner. Further reproduction prohibited without permission.

Figure 5

Heater Construction

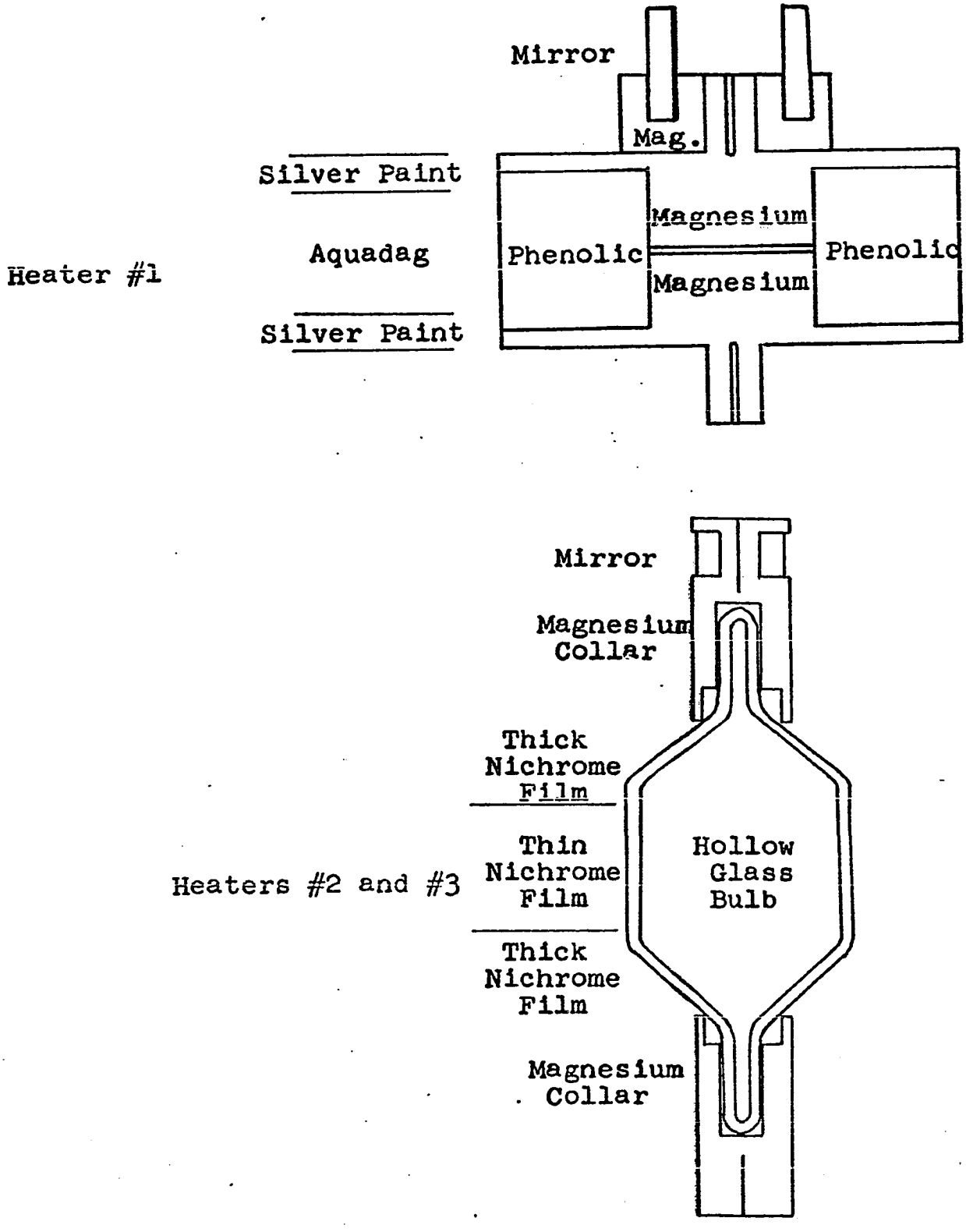

Reproduced with permission of the copyright owner. Further reproduction prohibited without permission.

the suspension wires.

The heaters are suspended from stainless steel wires of 0.0004", 0.0005", and 0.0007" diameters.[27] A smaller wire of 0.0002" Tungsten with a coating of Platinum, 25% by weight,[28] was attached to the bottom of the cylinder. This lower wire completed an electrical path and did not influence the period of oscillation which was determined by the larger upper wires.

In order to facilitate the assembly of the heater and suspension, the wires were first cut into lengths of about 2-1/2", and then both ends were soft soldered into hypodermic needle tubing (brass capillary tubing was also used on occasion). The hypodermic tubing varied in size from 0.0110" to 0.0125" O.D. and from 0.004" to 0.005" I.D. By attaching this relatively large tubing to the ends of the wires, they could be easily seen, and relatively easily glued (again with silver paint) into position in the suspension.

A drawing of the heater and suspension is shown in Figure 6. This entire suspension was attached to a rotatable shaft in the helium dewar as shown in Figure 3. Also shown in Figure 3 is a superconducting solenoid. It was used during the earlier work on the Hunt experiment

Reproduced with permission of the copyright owner. Further reproduction prohibited without permission.

Figure 6

CYLINDER SUSPENSION AND SUPPORT

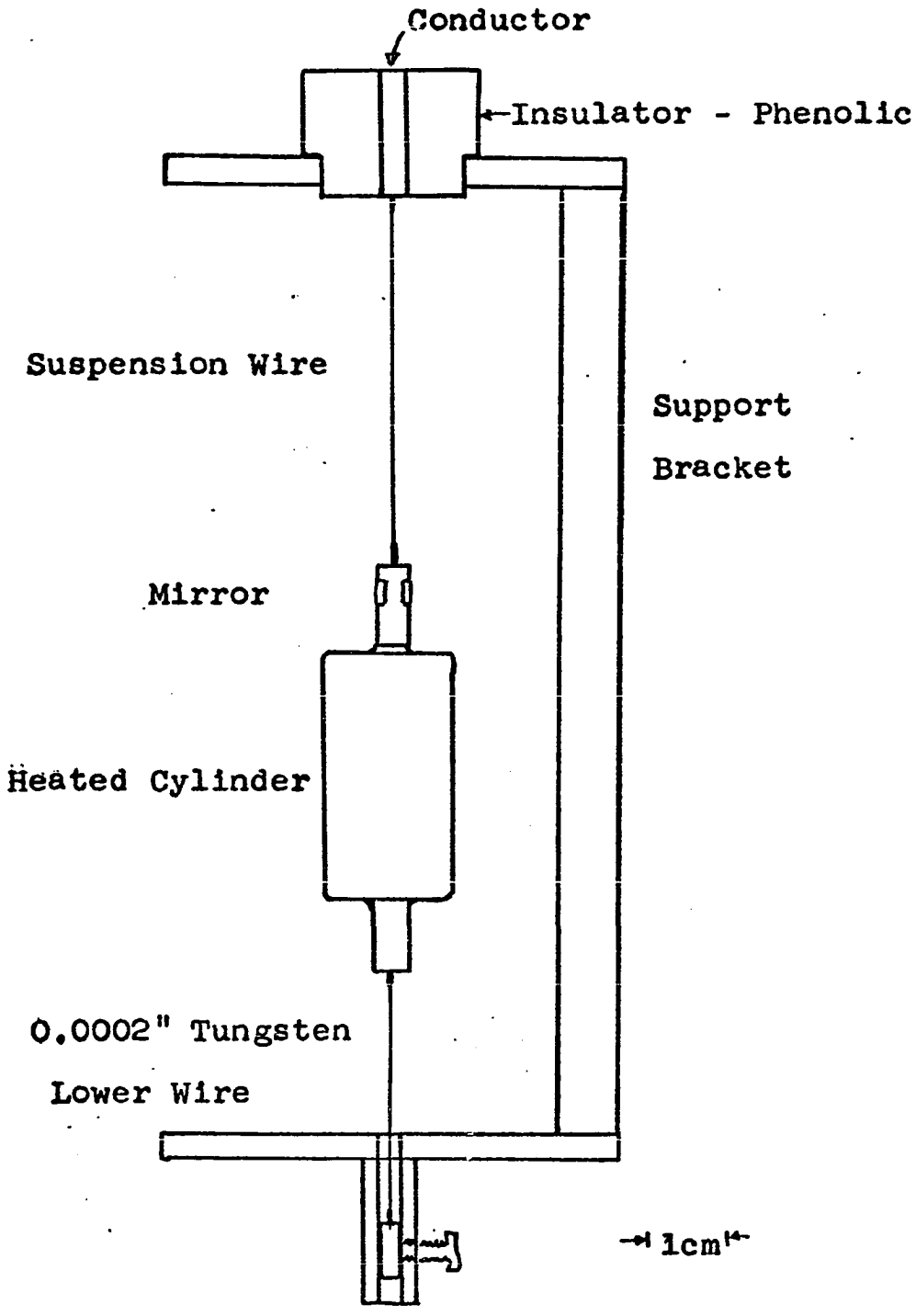

Reproduced with permission of the copyright owner. Further reproduction prohibited without permission.

to provide magnetic damping. It was noticed, however, that a magnetic field of the order of 100 gauss was sufficient to deflect the torsional pendulum a fraction of a radian. It was also noticed that this deflection was obtained without introducing a lateral displacement of the pendulum. This effect provided us with a very convenient means of achieving vibration free torsional displacements and we took advantage of it.

The amplitude of the torsional oscillations was detected by reflecting a light beam from a mirror attached to the oscillating cylinder onto a ground glass scale outside of the dewar. This arrangement is shown in Figure 7.

It should be noted that the projector was run at a reduced voltage for two reasons. First, it was then unnecessary to use a cooling fan, eliminating vibrations from that source. Second, the intensity of the beam was thereby reduced to a low level, reducing heat at the mirror to a minimum. We have estimated that the energy in the beam could not have been more than 1/2 milliwatt. Since this energy was incident on a portion of the apparatus which had a smaller radius than the portion we intentionally heated, and since only a small fraction

Reproduced with permission of the copyright owner. Further reproduction prohibited without permission.

DETECTION SCHEME

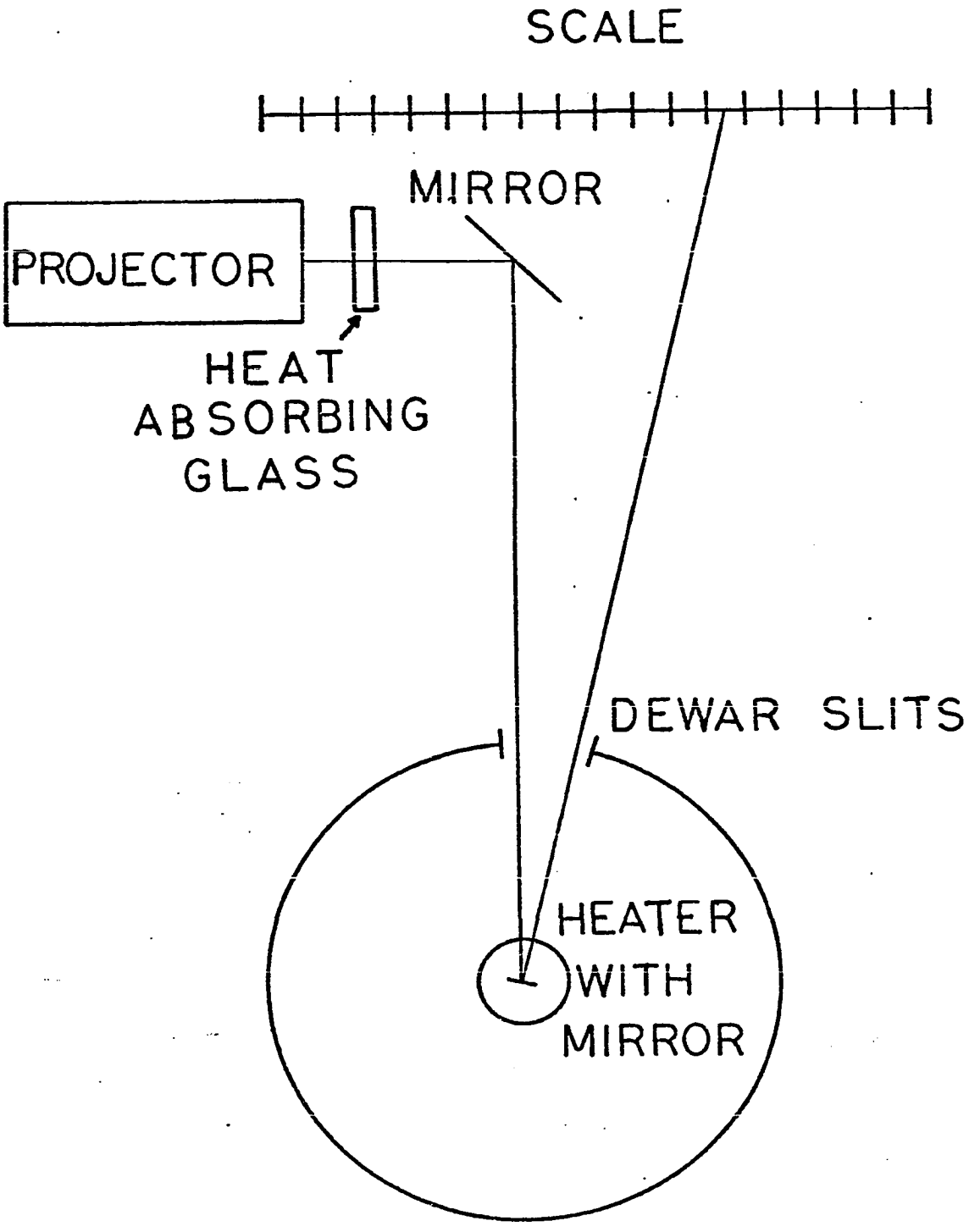

Figure 7

Reproduced with permission of the copyright owner. Further reproduction prohibited without permission.

of this power might have been absorbed by the mirror, we can be certain that the light spot had little or no effect.

Heat was supplied to the cylinders electrically. The apparatus required for this task is shown in Figure 8.

Procedure

The following procedure was used during a typical run to obtain measurements of the decrement over a range of power and over a range of temperature.

1. The temperature of the helium bath was set and held with the "Walker Regulator".[29] An hour was allowed for possible turbulence to subside.
2. The torsion pendulum was displaced by the application of a magnetic field in the range of 10 to 100 gauss.
3. The scale readings of the maxima of successive swings were recorded between a fixed range of amplitudes such that 40 plus or minus 10 oscillations were recorded. The scale readings were recorded to the nearest 0.2 mm. The largest amplitude swings observed were 1/30 rad.
4. Heat was applied and measured by passing a current through the resistive film on the heaters and observing the voltage drops scross a known resistor

Reproduced with permission of the copyright owner. Further reproduction prohibited without permission.

Figure 8

Electronics for Power Application and Measurement

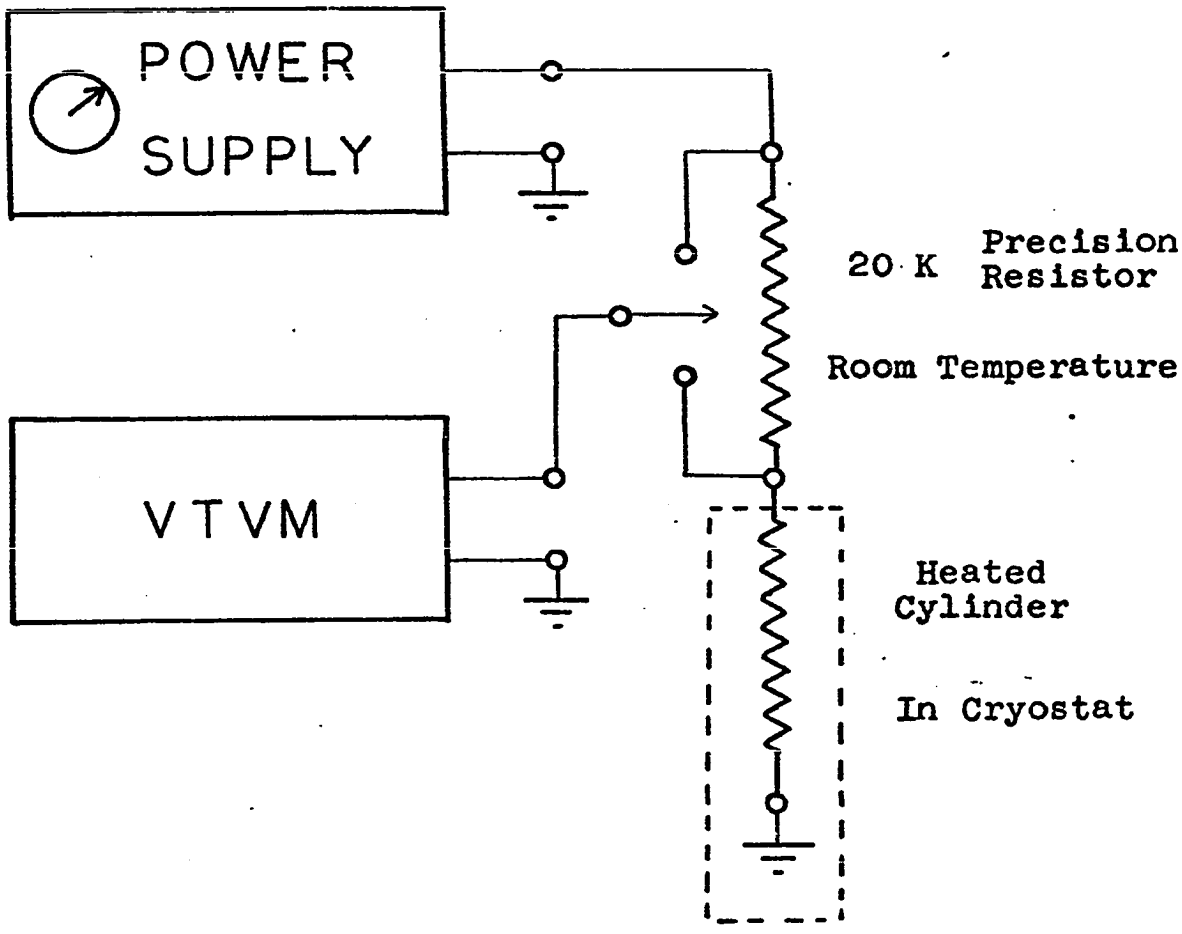

Power Supply: Lambda, Model LT2095A, 0-30 Volts

VTVM: Hewlett Packard, Model 410B

Reproduced with permission of the copyright owner. Further reproduction prohibited without permission.

and across the heated cylinder.

5. The pendulum was displaced by the magnetic field, and the field was turned off to allow free oscillations.
6. The amplitudes of swings through the same range of amplitudes explained in step 3 were recorded.
7. Steps 5 and 6 were repeated for the range of power to be explored at a given temperature.
8. The temperature was changed to another value, steps 1 to 7 were repeated, and this process was continued until the temperature range of interest was covered.

Usually the damping, at a given temperature, was recorded first for zero power and thereafter for increasing heater power. However, this procedure was sometimes reversed and occasionally random power points were taken to assure that the systematic procedure was not introducing a systematic error. Some points were repeated to determine the reproducibility of the experiment.

Reproduced with permission of the copyright owner. Further reproduction prohibited without permission.

Possible sources of error

Two of the steps in the experimental procedure which we have outlined were designed to minimize possible errors. Whenever the temperature was changed, an hour was allowed for turbulence to subside in the bath before measurements of the decrement were made. Also, the oscillations were observed over a fixed range of amplitudes so that the effects of unevenness in the glass of the dewars would be the same.

The temperature was maintained constant to better than 0.01 K, which might introduce a scatter of at most 1% of the zero power decrement.

The main source of error in the measurements of the changes in the decrement versus power is in the measurement of the power. The instrument used to measure the two voltages from which the power was determined was a Hewlett Packard 410 B VTVM. The manufacturer claims an accuracy of plus or minus 3% which we confirmed with a Fairchild digital voltmeter. The uncertainty in the power was then 6% and a reading error of 1% makes the total uncertainty in the power 8%.

One source of systematic error which was small, but which we eliminated, was the resistance of the

Reproduced with permission of the copyright owner. Further reproduction prohibited without permission.

suspension wires. Their resistances were measured, i.e. the resistance of a two inch piece of each different wire was measured, and subtracted from the resistance of the heater. This correction was at most 1/2%.

Finally, there is the error in the reading of the position of the light spot on the ground glass scale. That error is analyzed statistically, as explained in the following section, Data Analysis, and found to be much less than 1%.

Reproduced with permission of the copyright owner. Further reproduction prohibited without permission.

Data Analysis

The data as recorded consisted of a set of numbers corresponding to successive endpoints of swings of the pendulum. These numbers were punched onto computer cards and numerically analyzed to determine the logarithmic decrement. The Yale 7094/7040 DCS computer was used for this process. The program used is contained in Appendix II. A brief outline of the analysis is given below.

1. Read the sequence of amplitudes for a given decay.
2. Calculate the center of the oscillations by taking a running average of five swings.
3. Subtract the center value from the raw data and store the absolute value.
4. Take the logarithm of the results of 3.
5. From a least squares fit of the logarithms determine:
   a. The logarithmic decrement.
   b. The error in the decrement.
   c. The initial amplitude of the motion.

On a number of occasions we graphically displayed the data and compared a hand fit straight line to the computer fit line. This procedure not only gave a

Reproduced with permission of the copyright owner. Further reproduction prohibited without permission.

check on the computer program, but also allowed us to visually inspect the consistency of the straight line over less than the full range of decay. Figure 9 shows a curve of the logarithm of the amplitude versus cycle number for two of the data points contained in Figure 17. One of the curves is for zero power, the other is for a power of 7.42 milliwatts. The steeper slope can clearly be seen for the decay of the amplitude of oscillation with heater power applied. The line drawn through the data is the one determined by the computer program.

The error in the decrement determined in the data analysis program is actually the statistically probable error. It does not include any possible experimental uncertainties, nor does it reflect the reproducibility of the measurements. The probable error is calculated from the standard deviation of the log(A) from the computer fit value, using the relation [30]

$$\sigma_{DEC} = \sqrt{\frac{N'}{\Delta'}}\,\sigma_{LOG(A)}$$

where

$$\Delta' = N\sum_{i=1}^{N}(x_i)^2 - \left(\sum_{i=1}^{N} x_i\right)^2$$

Since $x_i = i$ for our case, it can be shown that the error

Reproduced with permission of the copyright owner. Further reproduction prohibited without permission.

Figure 9

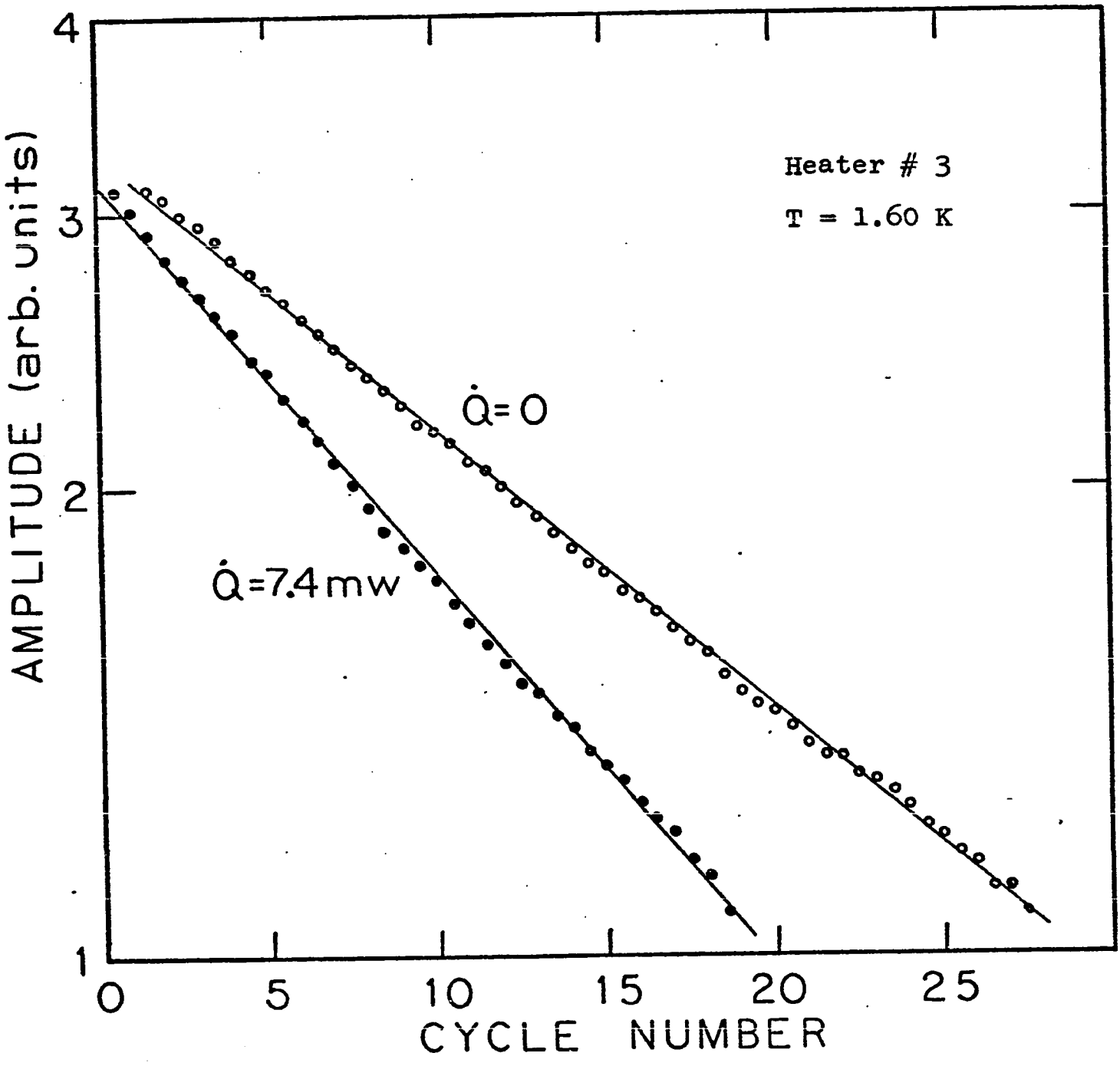

The logarithm of the absolute value of the endpoint of an oscillation is plotted versus the cycle number. The straight line is a computer fit to the data.

Reproduced with permission of the copyright owner. Further reproduction prohibited without permission.

is

$$\sigma_{DEC} = \sqrt{\frac{12}{N^3 - 3N}}\ \sigma_{LOG(A)}$$

Since N is always a large number, we can approximate

$$\sigma_{DEC} = \sqrt{\frac{12}{N^3}}\ \sigma_{LOG(A)}$$

The theoretical values for the zero power decrement and the change in decrement with power were also calculated numerically. The component of the decrement contributed by all forces other than the helium was measured for two experimental setups to be 2.3×10^{-3}, and that value is included in the "theoretical" value of the decrement. The other terms were calculated from the expressions which we have derived. The only term which requires slightly more than routine multiplication and division is the viscous contribution of the heated section of cylinder. The expression as derived in section II contains the term $Re\left\{\beta \frac{H_\alpha^{(1)}(\beta a)}{H_{H\alpha}^{(1)}(\beta a)}\right\}$. The magnitudes of α and $|\beta a|$ make the use of an assymptotic expression[31] for the Hankel functions valid only for zero power. By using the recursion relation $H_{\alpha-1}^{(1)}(\beta a) + H_{\alpha+1}^{(1)}(\beta a) = \frac{2\alpha}{\beta a} H_\alpha^{(1)}(\beta a)$,[32] the ratio can be reduced to a terminating continued fraction, the last term of which is $H_\epsilon^{(1)}(\beta a) / H_{H\epsilon}^{(1)}(\beta a)$, where $0 \leq \epsilon < 1$.

Reproduced with permission of the copyright owner. Further reproduction prohibited without permission.

This ratio can be computed using an assymptotic expression for the Hankel function. The computer program, which we have included in Appendix II, calculates the heated decrement by generating the terminating continued fraction, evaluating the last ratio with the first three terms of the assymptotic expression for the Hankel functions, and performing the necessary divisions to obtain the originally sought ratio. With additional arithmetic the zero power decrement, heated decrement, and changes in the decrement are calculated. These calculated values are displayed for comparison with the experimentally determined values on the figures in the following section.

Reproduced with permission of the copyright owner. Further reproduction prohibited without permission.

SECTION IV

Results, Discussion, and Conclusion

Oscillating Experiment Results and Discussion

On the succeeding pages are graphs of the results we obtained for our measurements of the logarithmic decrement of the three heaters #1, #2, and #3. For each heater, the temperature variation of the zero power decrement is shown followed by selective plots of the change in the decrement upon the application of heat. For each case, the data points are compared to a solid curve representing our calculated value for the damping or change in damping.

The first graph, Figure 10, is the zero power damping of heater #1. It does not agree well with our calculations, but we feel that the protruding mirrors caused this discrepency. The excellent agreement for the change in the decrement as a function of power (Figure 11) adds weight to the agrument that the mirrors provide the excess zero power damping. The zero power damping of the more streamlined heaters #2 and #3, shown in Figures 12 and 15 respectively, shows that our assumption of laminar flow is reasonable. The small deviations at the lowest temperatures on both of those curves is

Reproduced with permission of the copyright owner. Further reproduction prohibited without permission.

Figure 10

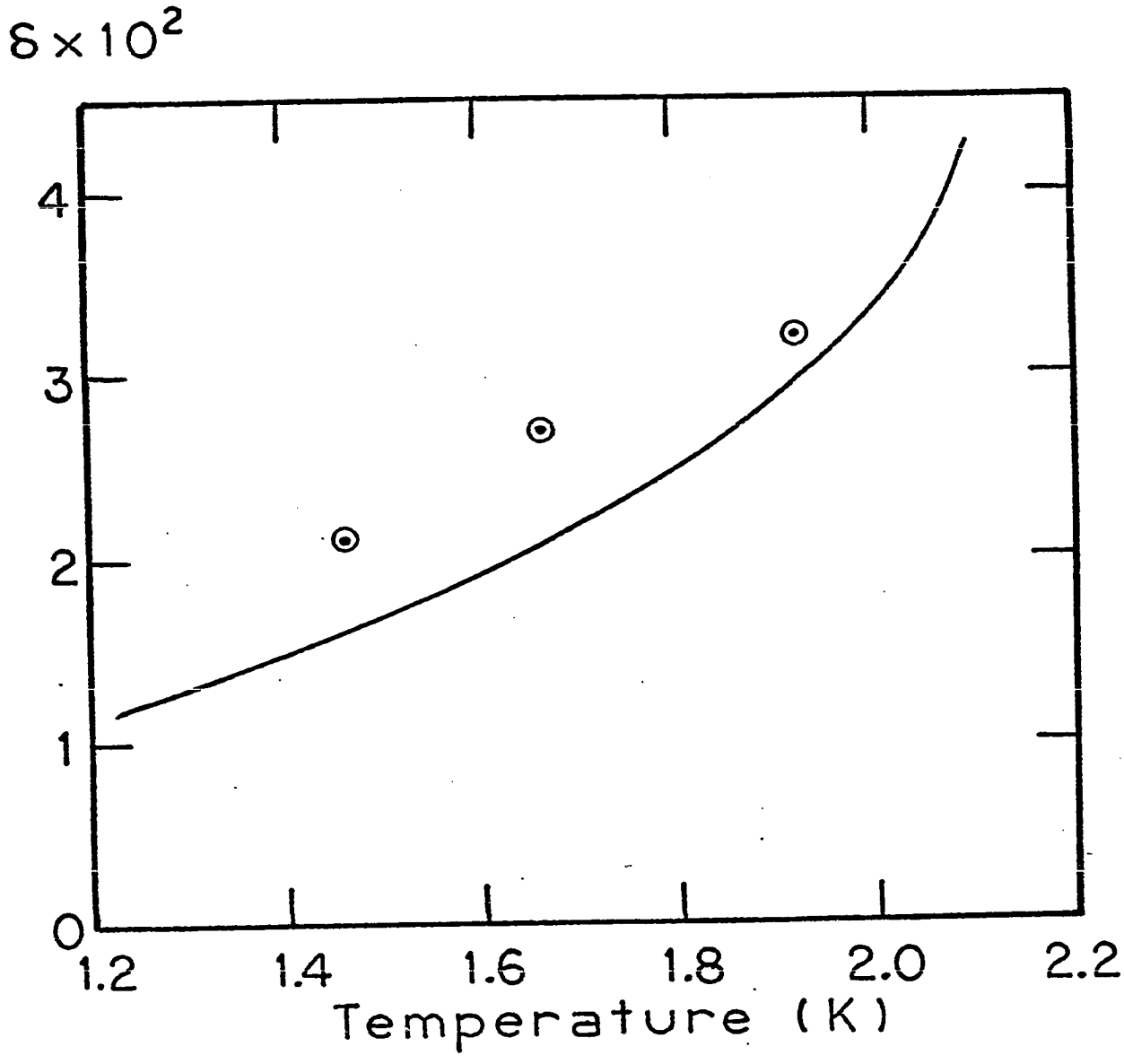

The zero power decrement versus temperature for Heater # 1 . P = 39 sec.

Reproduced with permission of the copyright owner. Further reproduction prohibited without permission.

Figure 11

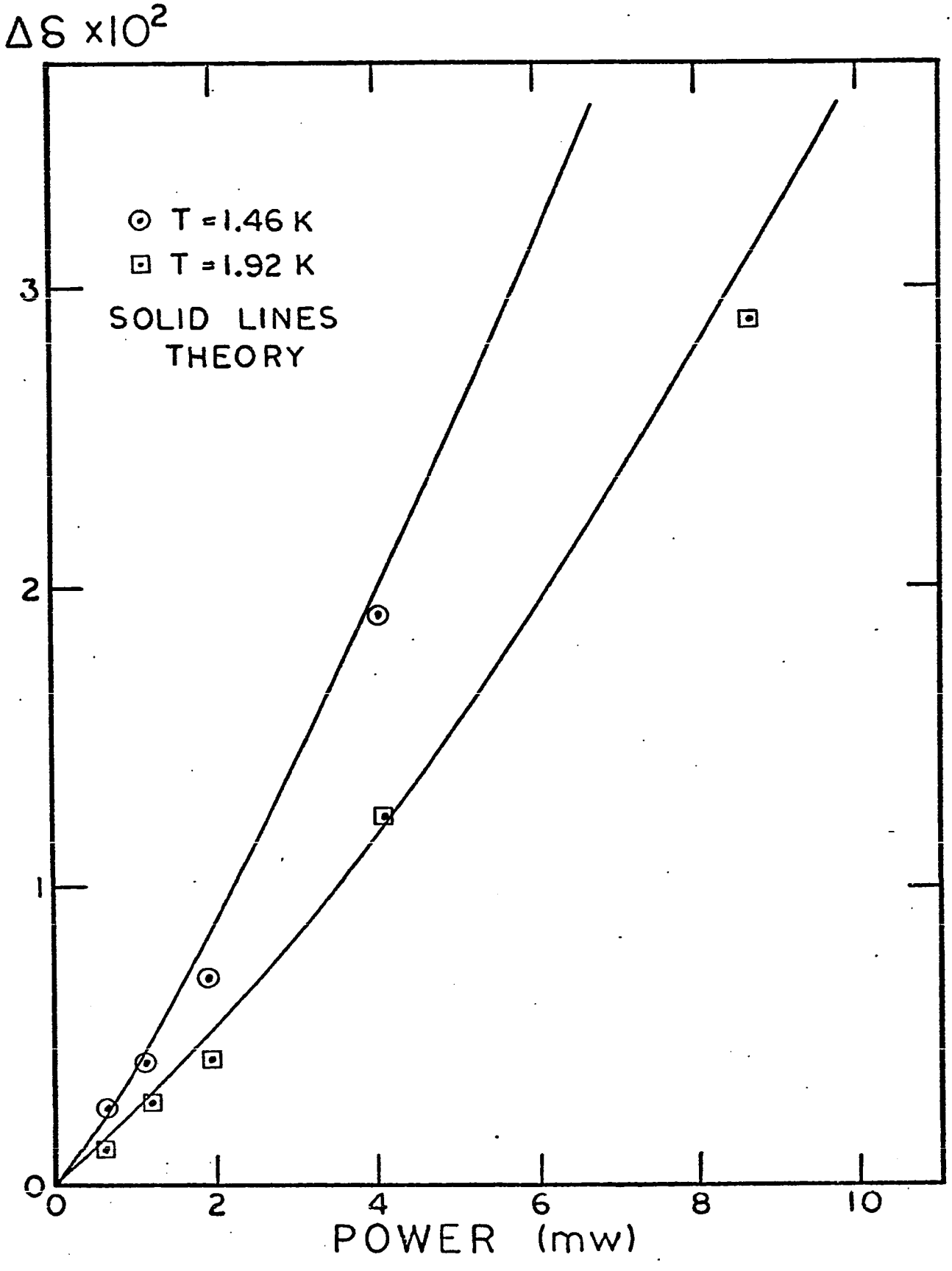

Δδ versus power for Heater # 1 . P = 39 sec.

Reproduced with permission of the copyright owner. Further reproduction prohibited without permission.

significant. There could be two possible reasons for these deviations. The first cause might be small vibrations of the cryostat. They could cause a disruption of the viscous waves and add to the damping. The other explanation could be the value of the viscosity which we used in our theoretical calculations. The viscosity of the normal fluid has been measured many times, and the agreement among the various investigators is notoriously poor. At 1.2 K differences of as much as 50% have been reported. We used the tabulated values of the viscosity in the recent book of Donnelly [33] in our calculations. We are unable fully to explain our discrepancy, but accept it as not too bad in light of the work of others on the viscosity. As we have mentioned, the zero power damping is displayed only to confirm our assumptions concerning the hydrodynamic flow.

The remaining curves display the change in the decrement as a function of power. While we have not up to now mentioned the fact, heaters #1, #2, and #3 represent successive generations of the experiment. The shorter two, #1 and #2 were used before we were fully aware that the normal viscous contribution to the decrement would be substantially modified by the application of

Reproduced with permission of the copyright owner. Further reproduction prohibited without permission.

Figure 12

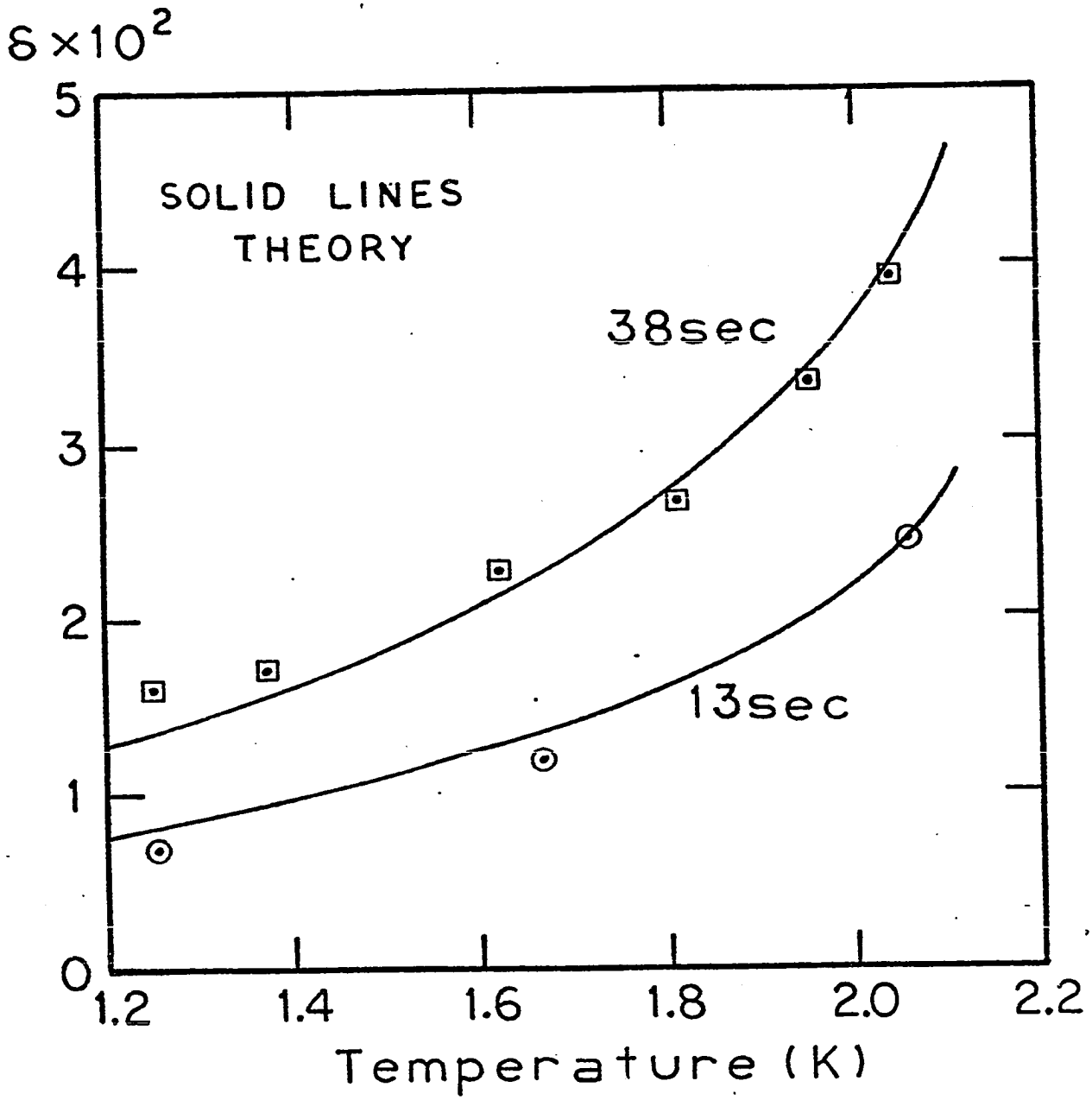

The zero power decrement versus temperature for Heater # 2 at two periods.

Reproduced with permission of the copyright owner. Further reproduction prohibited without permission.

Figure 13

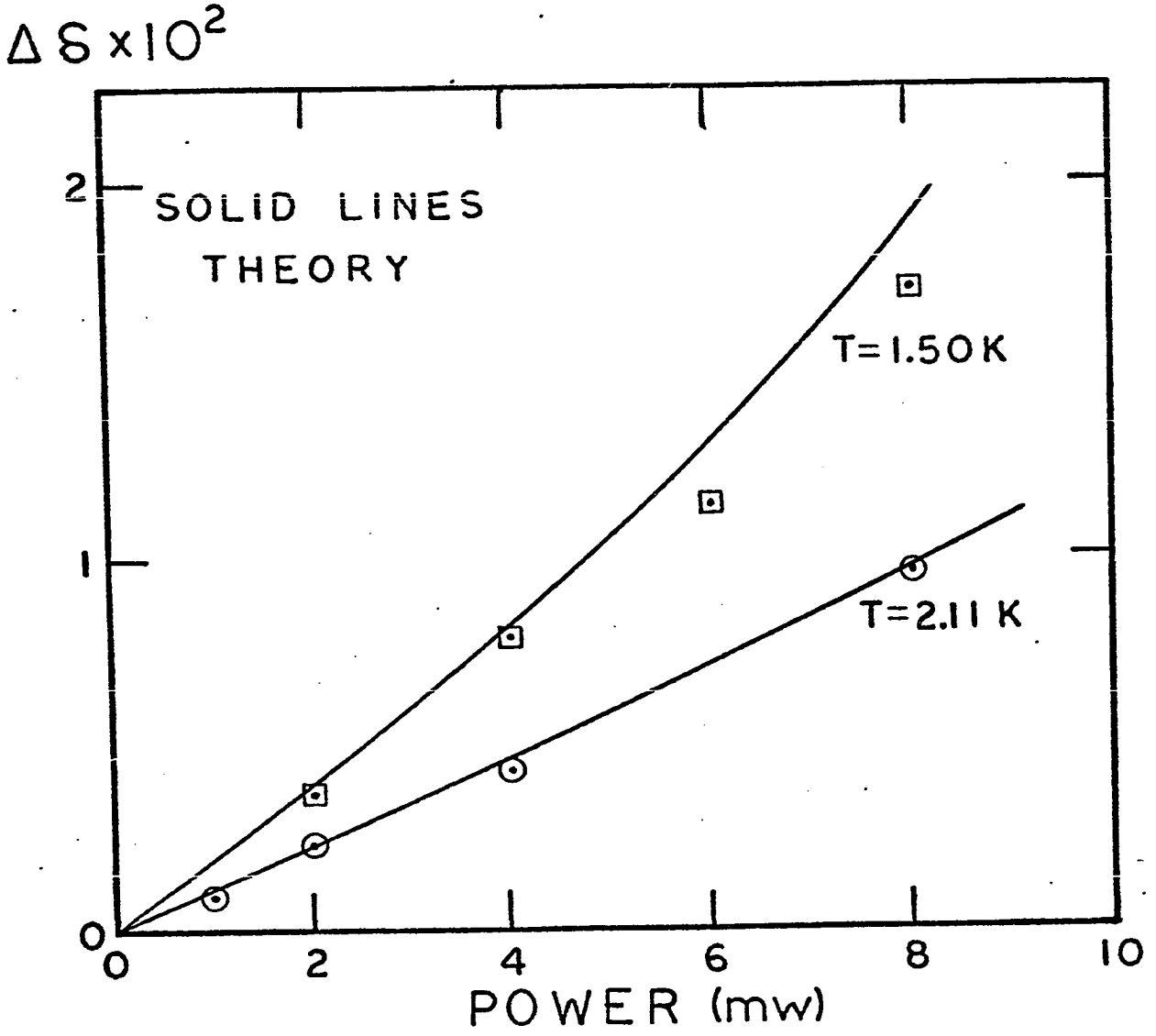

ΔS versus power for Heater # 2 . P = 26 sec.

Reproduced with permission of the copyright owner. Further reproduction prohibited without permission.

Figure 14

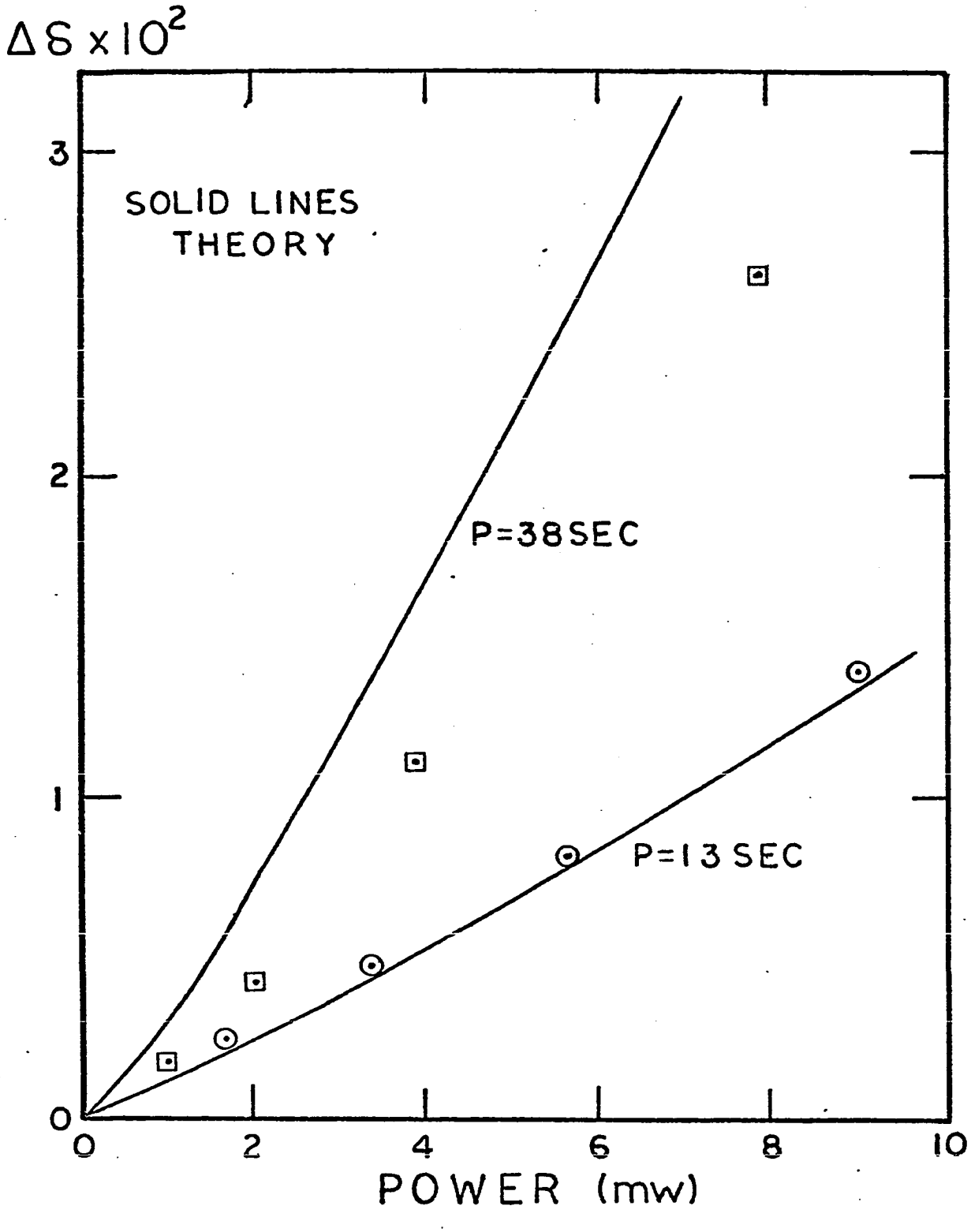

Δδ versus power for Heater # 2. T = 1.25 K.

Reproduced with permission of the copyright owner. Further reproduction prohibited without permission.

heat. The PO effect does not depend either on the uniformity of the heat or on end effects. The "stretched out" heater #3 is an attempt to reduce end effects and we would expect it to agree best with our calculations, which in fact it did.

The change in the decrement versus power was measured for only one period on heater #1. The data at two temperatures, 1.46 K and 1.92 K, are displayed on Figure 11. The agreement is almost surprising. Because the surface is rather rough, and because the heater is rather short, we might expect disagreement with our calculations of the normal viscous effects; but none arose.

The next two Figures 13 and 14 contain some of the data for the change in the decrement versus power for heater #2. Since our initial measurements of $\Delta\delta$ for heater #1 were lower than we expected, i.e. lower than the change which should be caused by the PO term alone, we felt that the rough surface might be dragging superfluid with it. This prompted the use of a glass bulb with an evaporated film for our second attempt. The fact that the data on $\Delta\delta$ for heater #2 was also lower than the PO term would predict prompted our more careful calculations. The improved theory shows agreement

Reproduced with permission of the copyright owner. Further reproduction prohibited without permission.

for periods of 13 sec (not displayed) over the entire temperature range, and for 26 sec (Figure 13), but all the data for a period of 38 sec is about 30% lower than our calculation. We can only suppose that end effects played a much more important part in the damping of the cylinder for this period (the viscous penetration depth is longer for a longer period) or that we made a systematic error in the measurement of the power for this set-up. In short, this data represents our "sore thumb".

In contrast to our "sore thumb", Figures 16 and 17 contain our best data. Heater #3 agrees consistently with our calculations both of the zero power damping and of $\Delta\delta$. Figure 16 shows the temperature variation of $\Delta\delta$ for a period of 26 sec. Except for larger scatter at the lower temperature, the agreement is excellent. Figure 17 shows the period dependance of $\Delta\delta$ versus power for a temperature of 1.60 K. Again, the agreement is excellent.

It should be noted that only representative data are plotted, and only that data is included in Appendix III. We have taken a good deal more data which agrees in some cases as well and in other cases as poorly as the data displayed.

Reproduced with permission of the copyright owner. Further reproduction prohibited without permission.

Figure 15

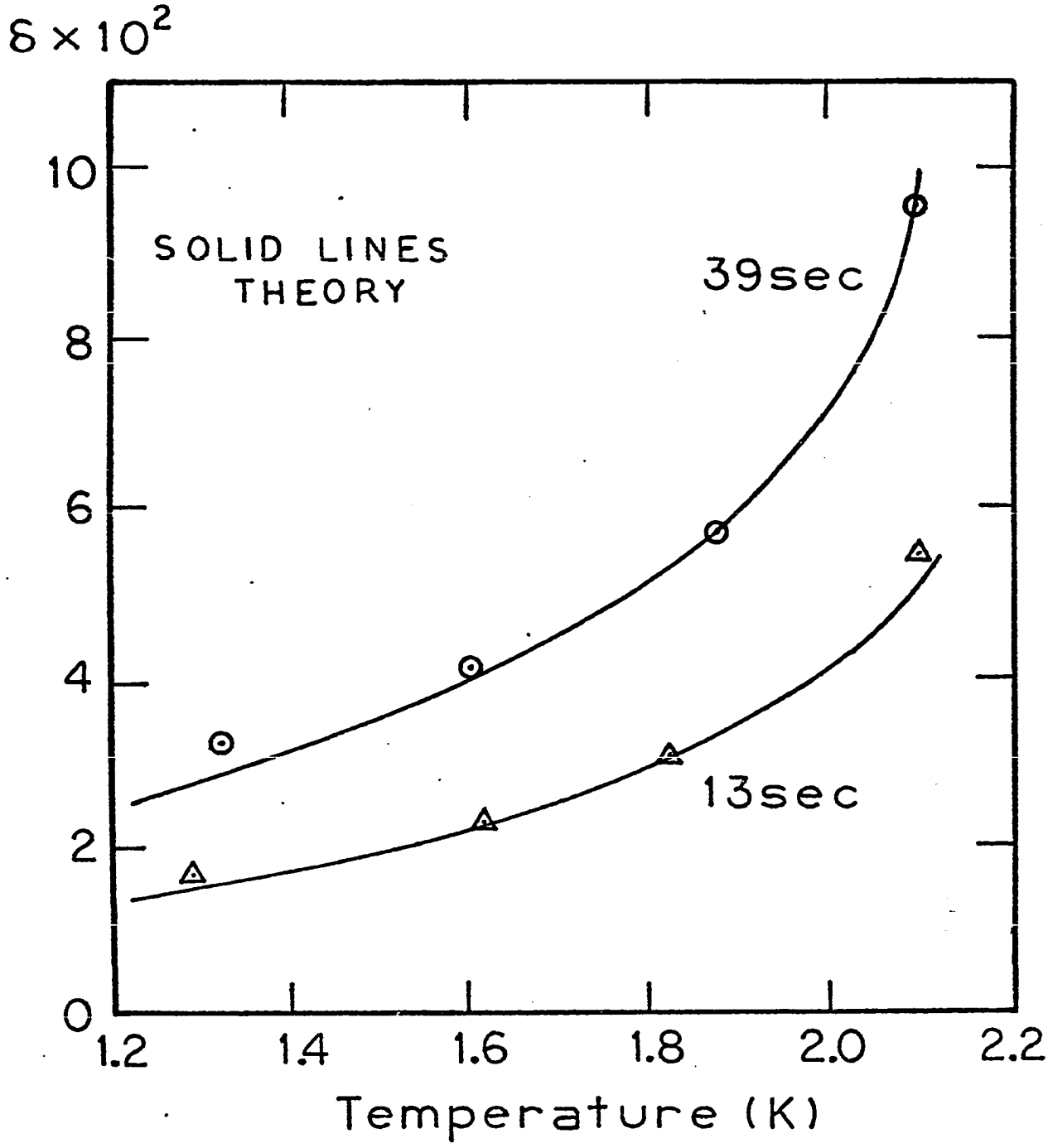

The zero power decrement versus temperature for Heater # 3 .

Reproduced with permission of the copyright owner. Further reproduction prohibited without permission.

Figure 16

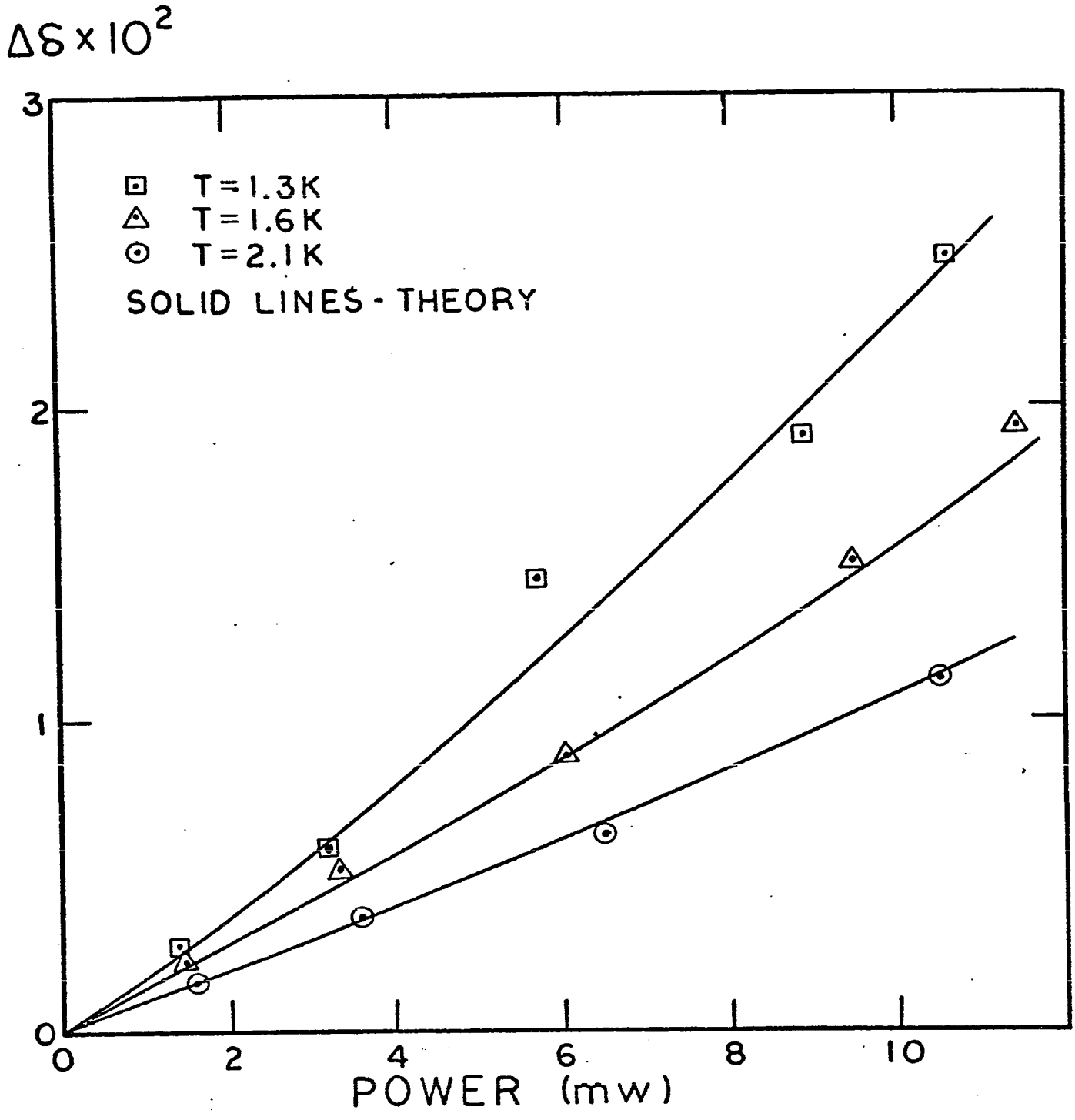

ΔS versus power for Heater # 3 . P = 26 sec.

Reproduced with permission of the copyright owner. Further reproduction prohibited without permission.

Figure 17

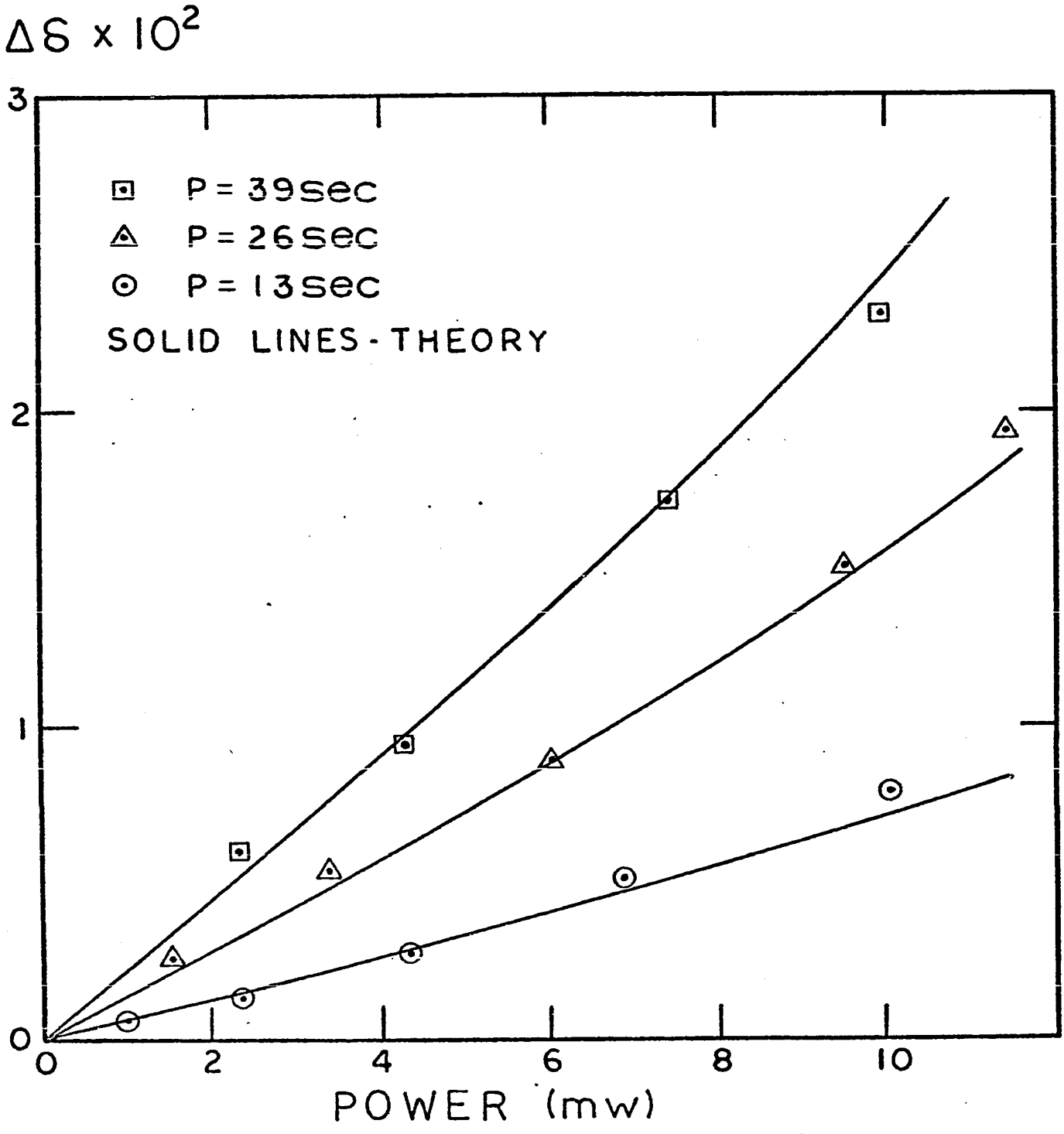

Δδ versus power for Heater # 3 . T = 1.6 K.

Reproduced with permission of the copyright owner. Further reproduction prohibited without permission.

Criticism of the Experiment of Hunt

During our repetition of the Hunt experiment, a thread of doubt began to grow concerning the validity of Hunt's[29] conclusions. We were observing spurious torques which were sometimes an order of magnitude and even more greater than the torques which Hunt had taken as his verification of the PO theory.

When calculating the normal viscous contribution to the decrement, we came upon another possible criticism of Hunt's experiment. The torque on the heated cylinder exerted by the normal fluid is given by the ϕr component of the momentum stress tensor.[23]

$$F_A = \eta \left(\frac{1}{r} \frac{\partial v_r}{\partial \phi} + \frac{\partial v_\phi}{\partial r} - \frac{v_\phi}{r} \right)$$

For a stationary cylinder, $v_\phi = 0$, however, for the experimental configuration which Hunt used, $\frac{\partial v_r}{\partial \phi} \neq 0$. He heated one side of a black cylinder with a beam of light.

Consider the following problem. A beam of light projects power such that one half of the beam has $\dot{q}$ power per unit area, the other half has $\dot{p}$ power per unit area. The beam is incident on a perfectly absorbing

Reproduced with permission of the copyright owner. Further reproduction prohibited without permission.

cylinder of radius "a" as shown below

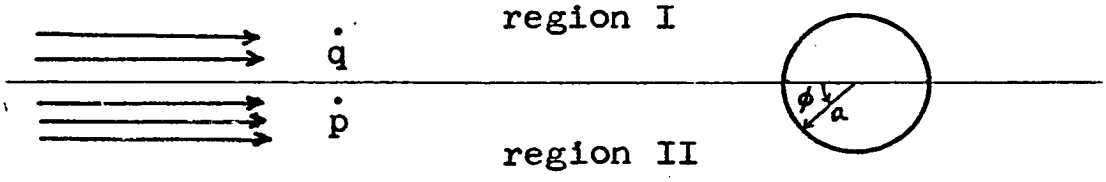

The power dissipated at the surface will be $\dot{q}\cos(\phi)$ for $0 > \phi > -\pi/2$, and $\dot{p}\cos(\phi)$ for $0 < \phi < \pi/2$. Assuming that the normal fluid created by the heat flows away perpendicular to the surface.

$$v_{nI} = \frac{\dot{q}\cos\phi}{\rho s T}\left(\frac{a}{r}\right) \equiv v_{qL}\left(\frac{a}{r}\right)\cos\phi$$

similarly,

$$v_{nII} = v_{pL}\left(\frac{a}{r}\right)\cos\phi$$

Then

$$F_n = \left(\eta\, v_{qL}\left(\frac{a}{r^2}\right)\frac{\partial\cos\phi}{\partial\phi}\right)\Big|_{r=a}$$

Integrating the force per unit area over the heated area, and calling the height of the cylinder h, we have

Reproduced with permission of the copyright owner. Further reproduction prohibited without permission.

$$\tau_I = \left(\eta v_{q\perp} \left(\frac{a}{r}\right) h \int_{-\frac{\pi}{2}}^{0} d\phi \, \frac{\partial \cos\phi}{\partial \phi} \right) \Big|_{r=a}$$

$$\tau_I = \eta v_{q\perp} h$$

similarly

$$\tau_{II} = -\eta v_{p\perp} h$$

$$\tau = \tau_I + \tau_{II} = \eta h \left(v_{q\perp} - v_{p\perp} \right)$$

In order to make a comparison with the data of Hunt we shall insert numbers into our expression for τ. h = 1 cm for Hunt's cylinders. Suppose $\dot{q}$ = 11 mw/cm^2 and $\dot{p}$ = 9 mw/cm^2. We have tabulated the torque as a function of temperature in Table 2.

Table 2 Torque from Assymetric Power

T (K)	η(poise)	$v_{q\perp} - v_{p\perp}$(cm/sec)	τ (dyne-cm)
1.2	14.9×10^{-6}	2.2×10^{-1}	3.2×10^{-6}
1.3	15.2×10^{-6}	1.3×10^{-1}	2.0×10^{-6}
1.5	13.5×10^{-6}	4.8×10^{-2}	6.4×10^{-7}
2.0	17.5×10^{-6}	7.4×10^{-3}	1.3×10^{-7}

The power densities while we have assumed correspond to a total power input of 2 mw, mid-range of the data of

Reproduced with permission of the copyright owner. Further reproduction prohibited without permission.

Hunt. Our calculated torque at 1.3 K is larger than all values which Hunt plots in one of his published graphs (Figure 3 in his P.R. article).

Considering our measurements of spurious torques much larger than any which Hunt measured, and the preceding calculation of another possible effect of the same magnitude as his torques, we can probably understand why Hunt was unable to distinguish the quantized levels of circulation in his experiment.

Reproduced with permission of the copyright owner. Further reproduction prohibited without permission.

Summary and Conclusions

As the title of this thesis implies, we have studied the role of heat as a tool for the measurement of superfluid velocites. Our study was initiated to confirm the prediction of Penney and Overhauser that measureable and time-independent torques should exist on heated bodies about which there exists a superfluid circulation. We proceeded in a straightforward way to try to set up persistent currents about a cylinder, heat it, and observe the predicted torques. Unfortunately, persistent currents are difficult to create reproducibly in volumes of helium of the size necessary for this experiment. Further complicating matters, we observed spurious torques on heated cylinders in HeII. While we did observe forces which were probably due to persistent currents, the inconsistency and the spurious torques make the usefulness of the technique questionable.

On the other hand we were able to prove that the effect predicted by Penney and Overhauser is real. By considering the case of a stationary superfluid and a moving heated surface, we have been able to determine experimentally all the parameters of the theory. After hydrodynamic corrections for the effects of heat flow on

Reproduced with permission of the copyright owner. Further reproduction prohibited without permission.

the viscous drag, we have compared our experiment to the predictions of the Penney Overhauser theory and found excellent agreement.

We feel that the PO effect is of seemingly limited use in the study of persistent currents, both for circulations of the order of a few quanta as studied by Hunt, and for persistent currents consisting of many hundreds of quanta as investigated here. However, we also feel that an extension of the oscillating cylinder experiment can in principle provide more information about the interaction of ρ_s with a solid surface. If the present experiment is extended to larger amplitudes, the superfluid should begin to interact with the surface. If the ρ_s interacts and is carried along by the surface, the PO effect should be diminished. Another extension of the oscillating experiment might be to carry the heat flow to the point at which the relative velocities of ρ_s and ρ_n cause an interaction. The ability to measure the decrement very accurately makes the oscillating pendulum an ideal candidate for the detection of the onset of the inteaction of the two components.

While our study verifies that the predicted momentum transfer does occur when a relative velocity exists between

Reproduced with permission of the copyright owner. Further reproduction prohibited without permission.

a heated surface and the superfluid component of HeII, other effects have limited its usefulness for studies of persistent currents. The effect may, however, prove useful for the study of the onset of the breakdown of superfluidity.

Reproduced with permission of the copyright owner. Further reproduction prohibited without permission.

APPENDIX I

Torsional Harmonic Oscillator

The following is a solution of the damped harmonic oscillator for torsional oscillations of a relatively undamped system. We present this solution to illustrate that if the logarithmic decrement of the damping is much less than unity, various contributions to the decrement can be separated and calculated separately using the approximate form of the decrement $\delta \approx \frac{\Delta E_{cycle}}{2E}$.

The motion is described by the differential equation

$$I\ddot{\theta} + R\dot{\theta} + k\theta = 0 \qquad \text{(I-1)}$$

The solution to this equation is of the form

$$\theta = Ce^{\gamma t} \qquad \text{(I-2)}$$

Substituting this form of the solution (I-2) into the differential equation (I-1), we have a quadratic equation for γ.

$$I\gamma^2 + R\gamma + k = 0 \qquad \text{(I-3)}$$

which has the solutions

$$\gamma = -\frac{R}{2I} \pm \sqrt{\frac{R^2}{4I^2} - \frac{k}{I}} \qquad \text{(I-4)}$$

Reproduced with permission of the copyright owner. Further reproduction prohibited without permission.

Assuming that $R^2/4I^2 < K/I$, we can write

$$\gamma = -\frac{R}{2I} \pm i\sqrt{\frac{k}{I}} \cdot \sqrt{1 - \frac{R^2}{4Ik}} \qquad \text{(I-5)}$$

The choice of sign in (I-5) as well as the value of the constant "C" in (I-2) depend on the initial conditions of the motion. If we specify that $\theta = \theta_o$ at $t = 0$, and we choose the minus sign for convenience we have

$$\theta = \theta_o e^{-\frac{\delta t}{P}} e^{-i\omega t} \qquad \text{(I-6)}$$

Where δ is the logarithmic decrement,

ω is the angular frequency,

P is the period, $P = 2\pi/\omega$.

If we further assume that

$$\frac{R^2}{4Ik} = n^2 \ll 1 \qquad \text{(I-7)}$$

we have

$$\omega = \sqrt{\frac{k}{I}} \qquad \text{(I-8)}$$

and

$$\delta = \frac{R}{2I} \cdot \sqrt{\frac{I}{k}} \cdot \frac{1}{2\pi} \qquad \text{(I-9)}$$

Combining (I-7) and (I-9) we have

$$\delta = \frac{n}{2\pi} \qquad \text{(I-10)}$$

Reproduced with permission of the copyright owner. Further reproduction prohibited without permission.

which indicates that our assumption (I-8) is equivalent to the condition

$$\delta << 1 \tag{I-11}$$

The equation for the motion is now

$$\theta = \theta_0 e^{-\frac{\delta t}{P}} e^{-i\omega t} \tag{I-12}$$

The energy stored in the oscillation is then

$$E = |\theta|^2 = \theta_0^2 e^{-\frac{2\delta t}{P}} \tag{I-13}$$

and

$$\frac{dE}{dt} = -\frac{2\delta}{P} \theta_0^2 e^{-\frac{2\delta t}{P}} \tag{I-14}$$

We can find the energy loss in a given cycle

$$\Delta E_{cycle} \approx -\frac{dE}{dt} \cdot P = 2\delta\theta_0^2 e^{-\frac{2\delta t}{P}} \tag{I-15}$$

and solving for δ we have

$$\delta = \frac{\Delta E_{cycle}}{2\theta_0^2 e^{-\frac{2\delta t}{P}}} \tag{I-16}$$

but

$$2E = 2\theta_0^2 e^{-\frac{2\delta t}{P}} \tag{I-17}$$

Reproduced with permission of the copyright owner. Further reproduction prohibited without permission.

hence,

$$\delta = \frac{\Delta E_{cycle}}{2E} \qquad \text{(I-18)}$$

We can now say that if we know that $\delta \ll 1$, and we know the drag force on the oscillator, we can calculate the logarithmic decrement from (I-18).

Furthermore, we recall that

$$\delta = \frac{R}{2I} \cdot \sqrt{\frac{I}{k}} \cdot \frac{1}{2\pi} \qquad \text{(I-19)}$$

Hence, should two or more drag forces be present, i.e. $R = R_1 + R_2 + R_3 + \cdots$, we can calculate the contribution to the decrement from each separately, because (I-9) is linear in R .

Reproduced with permission of the copyright owner. Further reproduction prohibited without permission.

APPENDIX II

Computer Programs

The following four pages contain two programs, one of which we used to analyze the raw data, and the other we used to perform the calculations necessary for making our theoretical predictions.

Reproduced with permission of the copyright owner. Further reproduction prohibited without permission.

PROGRAM FOR DATA ANALYSIS

```
      REAL RNDP,OVAL,SUMX,SUMY,SUMXY,DEC,B,SSQEV,T,P,QMW,SDEV,XI,SUMXX
      INTEGER I,N,NDK,NDP,NI
      DIMENSION DATA(200), DATSM(200),DTSL(200), DEV(200)
      DIMENSION  TK(50)  ,DC(50)  ,Q(50)
      DIMENSION  RMKS(50)
      DIMENSION A(100)
C     START BY READING NUMBER OF DECKS
      READ(5,201) NDK
  201 FORMAT(I4)
      READ(5,202) YK
  202 FORMAT(E11.4)
C     LARGE DO LOOP FOR EACH CURVE
      DO 101 N=1,NDK
      READ(5,201)NDP
      M = NDP - 1
       DO  1 I = 1,M,2
       READ (5,200) DATA(I), DATA(I+1)
  200  FORMAT (2F6.0)
    1  CONTINUE
      OVAL=0.1*(DATA(1)+DATA(3)+DATA(5)+DATA(7)+DATA(9))
     1+0.125*(DATA(2)+DATA(4)+DATA(6)+ DATA(8))
C     DO THE FIRST SUBTRACTIONS
      DO 303 I=1,6
  303 DATSM(I)=ABS(DATA(I)-OVAL)
C     DO THE MIDDLE SUBTRACTIONS
      NI=NDP-6
      DO 306 I=7,NI,2
      OVAL=OVAL-0.1*(DATA(I-6)-DATA(I+4))-0.125*(DATA(I-5)-DATA(I+3))
      DATSM(I)=ABS(DATA(I)-OVAL)
  306 DATSM(I+1)=ABS(DATA(I+1)-OVAL )
C     DO THE END POINT SUBTRACTIONS
      DO 307 I= NI,NDP
  307 DATSM(I)=ABS(DATA(I)-OVAL)
C     COMPUTE THE LOGS OF AMPLITUDES
      DO 309 I=1,NDP
  309 DTSL(I)=ALOG(DATSM(I))
C     START THE CURVE FIT SUMS
      RNDP=NDP
      SUMX = RNDP*(RNDP+1.0)/2.0
      SUMXX=0.0
      SUMY=0.0
      SUMXY=0.0
C     COMPUTE THE SUMS
      DO 308 I=1,NDP
      XI=I
      SUMXX=SUMXX+XI*XI
      SUMY=SUMY+DTSL(I)
  308 SUMXY=SUMXY+XI*DTSL(I)
C     COMPUTE THE SLOPE, ZERO VALUE, AND LOG DEC
      DEC=((RNDP*SUMXY)-(SUMX*SUMY))/((RNDP*SUMXX)-(SUMX*SUMX))
      B = (SUMY - DEC*SUMX)/RNDP
```

Reproduced with permission of the copyright owner. Further reproduction prohibited without permission.

```
C       COMPUTE DEVIATIONS
        DO 600 I=1,NDP
        XI=I
  600 DEV(I)=DTSL(I) - B - (XI*DEC)
C       COMPUTE SDEV
        SSQEV=0.0
        DO 601 I=1,NDP
  601 SSQEV=SSQEV + (DEV(I)*DEV(I))
        SDEV=SQRT(SSQEV/RNDP)
        DEC = 2.0*DEC
        READ (5,500) T,P,QMW
  500 FORMAT (3F7.2)
        C = NDP
        A(N)=(C*(C+1.0)*((2.0*C)+1.0)/6.0)-(C*(C+1.0)*(C+1.0)/4.0)
        A(N) = SDEV/SQRT(A(N))
C       PRINT OUT SINGLE NUMBERS
        WRITE(6,501)  T,P,QMW,B,DEC,SDEV    ,A(N)
  501 FORMAT (1H1 ,4HT = , F5.2,5X,4HP = ,F7.2,5X,6HQMW = ,F5.2,5X,
     1 4HB = ,E12.5,5X,6HDEC = ,E12.5,5X,7HSDEV = ,E12.5,5X,7HERROR= ,
     2E10.3,//)
C       PRINT OUT OF DATA COLUMNS
        WRITE (6,502)
  502 FORMAT (1H0, 6H DATA ,5X,6H AMPL ,5X,8H LOG(A)    ,5X,7H DIFF  //)
        WRITE (6,503)(DATA(I),DATSM(I),DTSL(I),DEV(I),I=1,NDP)
  503 FORMAT (1H ,F6.0,5X,F6.0,5X,F8.5,5X,F9.6)
C        STORE VALUES NEEDED FOR THE SUMMARY
        DC(N) = DEC
        TK(N) = T
        Q(N) = QMW
  101 CONTINUE
C       PRINT ANY REMARKS ABOUT THE RUN AT THE HE AD OF THE SUMMARY
        READ(5,800)  (RMKS(I) , I = 1,20)
  800 FORMAT (20A4)
        WRITE(6,801) (RMKS(I) , I = 1,20)
  801 FORMAT(1H1,///20A4,///)
C       WRITE THE HEADINGS FOR THE SUMMARY
        WRITE(6,702)
  702 FORMAT(1H0, 4X, 1HT, 19X, 1HQ, 18X, 3HDEC, 15X, 9HD-HEAT-EX,
     1 11X, 9HD-HEAT-TH,/)
C       WRITE THE FIRST VALUES OF T, Q, AND DEC
        WRITE(6,701) TK(1), Q(1), DC(1)
  701 FORMAT ( 1H0,/3X, F5.2, 15X, F5.2, 12X, E12.5)
        DOT = DC(1)
C       DO LOOP TO ASSEMBLE AND PRINT OUT THE SUMMARY
        M = NDK - 1
        DO 507 I = 1,M
        IF ( TK(I) -TK(I+1))  506,505,506
  505 DEX = DOT - DC(I+1)
        DTH = YK * Q(I+1) / TK(I+1)
        WRITE(6,700) TK(I+1), Q(I+1), DC(I+1) , DEX, DTH
  700 FORMAT(1H0, 2X, F5.2, 15X, F5.2, 12X, E12.5, 9X, E10.3, 10X,E10.3)
        GO TO 507
  506 WRITE(6,701) TK(I+1), Q(I+1), DC(I+1)
        DOT = DC(I+1)
  507 CONTINUE
        WRITE(6,802)
  802 FORMAT (1H1)
        STOP
        END
$DATA
```

Reproduced with permission of the copyright owner. Further reproduction prohibited without permission.

PROGRAM FOR THEORETICAL PREDICTION OF DECREMENT

```
      COMPLEX H1, H2, C1I, C1R, B, HRAT, U, V, Z, C, G ,H
      DIMENSION EN(20), RN(20), VN(20), AL(20), DVS(20), DPO(20),
     1 DEC(20), DDEC(20),CMNTS(20)
      REAL Y, A, D, E, SN, PI, PER, DOV, T, XI, LM, DVT, GNU, W, Q,
     1 AREA, XM, AL1, X
      COMMON  B,C1R,C1I,A
C     START BY READING THE TEMPERATURE DEPENDANT PARAMETERS
  101 FORMAT(E10.3)
      READ(5,101) (RN(I), I=2,11)
      READ(5,101) (EN(I), I=2,11)
      SN = +0.172E+04
      PI = 3.141592
C     READ THE GEOMETRY OF THE SAMPLE
  777 READ (5,102) Y, A, D, E
  102 FORMAT(F7.4)
C     READ THE PARAMETERS OF A GIVEN RUN
      READ (5,102) PER
      READ (5,101) DOV
      READ(5,108) (CMNTS(I),I=1,20)
  108 FORMAT(20A4)
      AREA = 2.0*PI*A*D*E
C     WRITE THE GEOMETRICAL PARAMETERS
      WRITE(6,109) (CMNTS(I),I=1,20)
  109 FORMAT(1H1,20A4)
      WRITE (6,104) Y,A,D,E,AREA
  104  FORMAT (1H0, 3HI= , F6.3,5X, 3HA= , F6.3, 5X, 3HD= , F6.3, 5X,
     1 3HE= , F6.3, 5X, 5HAREA=, F6.3/)
      WRITE (6,105) PER
  105 FORMAT (1H0,3HP= ,F6.3/)
      W = 2.0*PI/PER
      DO 20 I=2,11
      GNU = EN(I)/RN(I)
      XI=I
      T = 1.0 + 0.1*XI
      LM = SQRT(2.0*GNU/W)
      C1R = CMPLX (1.0,0.0)
      C1I = CMPLX(0.0,1.0)
      B = CMPLX(1.0/LM,1.0/LM)
      DVT = ((PI**2*A**4*EN(I))/(LM*W*Y))*(1.0+(1.0-E)*((2.0*D/A) +
     1 (3.0*LM*D/A**2)))
      WRITE (6,106) T,DVT,LM,GNU,DOV
  106  FORMAT(1H0,3HT= ,F6.3,5X,5HDVT= ,E10.3,5X,3HLM=,E10.3,5X,
     1 5HGNU= ,E10.3,5X,5HDOV= ,E10.3/)
      DO 30 J=1,11
      Q=J-1
      VN(J) = Q/(AREA*RN(I)*SN*T)
      AL(J) = (VN(J)*A)/(2.0*GNU)
      XM = 0.0
```

Reproduced with permission of the copyright owner. Further reproduction prohibited without permission.

```
    3 XM=XM+1.0
      AL1 = AL(J) - XM
      IF(AL1) 1,2,3
    1 XM = XM - 1.0
      AL1 = AL1 + 1.0
    2 H1 = H(AL1)
      H2=H(1.0+AL1)
      HRAT = (H1/H2)*C1I
      X = XM
      IF (X) 4,4,5
    4 Z = B*HRAT
    8 GO TO 7
    5 V =HRAT
    9 U = CMPLX (2.0*(AL(J) + 1.0 - X),0.0)
      V=U/(B*A)-V
      V=C1R/V
      Z=V*B
      X=X-1.0
      IF(X) 8,8,9
    7 C = CMPLX(2.0/A,0.0)
      G = C-Z
      DVS(J) = 2.0*PI**2*A**3*D*E*EN(I)*REAL(G)/(W*Y)
      DPO(J) = PER*Q*A**2/(2.0*SN*Y*T)
      DEC(J) = DVS(J) + DPO(J) + DVT + DOV
   30 DDEC(J) = DEC(J) - DEC(1)
      WRITE (6,107) ((VN(J),J=1,11),(AL(J),J=1,11),(DVS(J),J=1,11),(DPO
     1(J),J=1,11),(DEC(J),J=1,11),(DDEC(J),J=1,11))
  107 FORMAT(1H0,5HVN    ,11E11.3/,6HALPHA ,11E11.3/,6HDVS    ,11E11.3/,
     16HDPO    11E11.3/,6HDEC    ,11E11.3/,6HDDEC   ,11E11.3/)
   20 CONTINUE
      GO TO 777
  888 STOP
      END
      COMPLEX FUNCTION H(P)
      COMPLEX N1, N2, D1, D2 ,B,C1R,C1I
      REAL P , A
      COMMON  B,C1R,C1I,A
      N1 = CMPLX    (4.0*P*P-1.0,0.0)
      N2 = CMPLX    ((4.0*P*P-1.0)*(4.0*P*P-9.0),0.0)
      D1= 8.0*C1I*B*A
      D2 = 128.0*B*B*A*A
      H = C1R - (N1/D1) - (N2/D2)
       RETURN
      END
$DATA
```

Reproduced with permission of the copyright owner. Further reproduction prohibited without permission.

APPENDIX III

Data

This appendix contains the data which is plotted in Figures 9 through 17 in the thesis. The first two pages (83 & 84) contain the data which was plotted in Figure 9. For the rest of the data, the Figures in which they are plotted are indicated.

Since the computer doesn't read and write Greek symbols, it is necessary to label the parameters of the experiment differently in the computer programs and resultant printout. The following list serves as a translational table from the computer printout to the notation used in the text of this thesis.

T = T, P = P, QMW = Q = $\dot{Q}$, DEC = δ

B = amplitude of oscillation at t = 0.

SDEV = standard deviation of the data from the computer fit line.

ERROR = statistical error in the decrement. = σ_{DEC}

DATA = raw data as recorded from ground glass scale.

AMPL = absolute value of the raw data minus the position on the ground glass scale of the center of the oscillations.

Reproduced with permission of the copyright owner. Further reproduction prohibited without permission.

LOG(A) = natural logarithm of AMPL.

DIFF = difference between the data and the computer fit line for each data point.

D-HEAT-EX = the experimental value of $\Delta\delta$.

Reproduced with permission of the copyright owner. Further reproduction prohibited without permission.

T = 1.60 P = 39.32 QMW = 0. B = 0.57504E 01

DEC = -0.40542E-01 SDEV = 0.11186E-01 ERROR= 0.877E-04

DATA	AMPL	LOG(A)	DIFF
1058.	311.	5.73947	0.009328
1676.	307.	5.72717	0.017301
1070.	299.	5.70011	0.010508
1664.	295.	5.68731	0.017984
1080.	289.	5.66608	0.017021
1650.	281.	5.63871	0.009921
1092.	276.	5.62203	0.013512
1638.	270.	5.59675	0.008507
1104.	264.	5.57595	0.007972
1626.	258.	5.55296	0.005254
1116.	252.	5.52883	0.001399
1614.	246.	5.50594	-0.001223
1128.	240.	5.48043	-0.006463
1604.	236.	5.46404	-0.002579
1136.	232.	5.44652	0.000170
1594.	226.	5.42076	-0.005324
1148.	220.	5.39272	-0.013092
1586.	218.	5.38541	-0.000127
1154.	214.	5.36457	-0.000695
1576.	208.	5.33898	-0.006018
1162.	206.	5.32812	0.003392
1568.	200.	5.29807	-0.006388
1172.	196.	5.27811	-0.006071
1560.	192.	5.25750	-0.006418
1182.	187.	5.22923	-0.014409
1552.	183.	5.21140	-0.011975
1190.	179.	5.18934	-0.013763
1546.	177.	5.17417	-0.008660
1198.	172.	5.14808	-0.014485
1540.	170.	5.13521	-0.007078
1204.	167.	5.11739	-0.004624
1534.	163.	5.09436	-0.007383
1212.	159.	5.07047	-0.011002
1528.	157.	5.05465	-0.006553
1220.	152.	5.02157	-0.019361
1520.	148.	4.99958	-0.021089
1226.	146.	4.98395	-0.016445
1516.	144.	4.96947	-0.010655
1232.	141.	4.94556	-0.014290
1510.	137.	4.92326	-0.016319
1238.	135.	4.90786	-0.011447
1508.	135.	4.90268	0.003641
1242.	132.	4.88394	0.005168
1504.	130.	4.86638	0.007884
1248.	127.	4.84576	0.007532
1500.	125.	4.82671	0.008758
1254.	122.	4.80402	0.006334
1496.	120.	4.78749	0.010079
1260.	117.	4.76046	0.003318
1492.	115.	4.74667	0.009799
1266.	111.	4.71313	-0.003477
1488.	111.	4.70592	0.009591
1270.	107.	4.67656	0.000498

Reproduced with permission of the copyright owner. Further reproduction prohibited without permission.

T = 1.60 P = 39.31 QMW = 7.42 B = 0.57500E 01

DEC = -0.57642E-01 SDEV = 0.14285E-01 ERROR= 0.182E-03

DATA	AMPL	LOG(A)	DIFF
1050.	312.	5.74428	0.023077
1664.	302.	5.70910	0.016715
1070.	292.	5.67812	0.014557
1644.	282.	5.64049	0.005743
1088.	274.	5.61459	0.008663
1620.	266.	5.58199	0.004889
1104.	259.	5.55779	0.009511
1616.	253.	5.53240	0.012940
1122.	242.	5.48894	-0.001702
1602.	238.	5.47227	0.010452
1136.	229.	5.43197	-0.001024
1586.	221.	5.39997	-0.004206
1150.	215.	5.37064	-0.004718
1572.	207.	5.33272	-0.013816
1164.	201.	5.30380	-0.013912
1560.	195.	5.27249	-0.016406
1178.	188.	5.23591	-0.024163
1550.	184.	5.21548	-0.015772
1188.	179.	5.18683	-0.015604
1542.	175.	5.16536	-0.008252
1199.	169.	5.12990	-0.014890
1532.	164.	5.09987	-0.016101
1210.	159.	5.06890	-0.018243
1524.	155.	5.04343	-0.014900
1220.	150.	5.01030	-0.019203
1518.	148.	4.99755	-0.003133
1228.	143.	4.96109	-0.010769
1512.	141.	4.95053	0.007490
1235.	136.	4.91632	0.002103
1504.	133.	4.88658	0.001184
1242.	130.	4.87061	0.014027
1498.	126.	4.83310	0.005345
1250.	123.	4.81543	0.016493
1494.	121.	4.79248	0.022365
1259.	116.	4.74970	0.008407
1488.	113.	4.73136	0.018890
1268.	107.	4.66861	-0.015040
1482.	107.	4.67703	0.022195
1274.	101.	4.61065	-0.015358
1476.	101.	4.61957	0.022377
1280.	95.	4.54913	-0.019242
1470.	95.	4.55860	0.019056

Reproduced with permission of the copyright owner. Further reproduction prohibited without permission.

DATA PLOTTED FOR HEATER *1* IN FIGURES 10 AND 11

T	Q	DEC	D-HEAT-EX
P=39sec			
1.92	0.	-0.32325E-01	
1.92	0.62	-0.33520E-01	0.120E-02
1.92	1.22	-0.34998E-01	0.267E-02
1.92	1.95	-0.37236E-01	0.491E-02
1.92	4.10	-0.44595E-01	0.123E-01
1.92	8.71	-0.61246E-01	0.289E-01
1.66	0.	-0.27355E-01	
1.46	0.	-0.21304E-01	
1.46	0.63	-0.22328E-01	0.102E-02
1.46	1.17	-0.25399E-01	0.410E-02
1.46	1.93	-0.28156E-01	0.685E-02
1.46	4.04	-0.40254E-01	0.190E-01
1.46	8.67	-0.70287E-01	0.490E-01

Reproduced with permission of the copyright owner. Further reproduction prohibited without permission.

DATA PLOTTED FOR HEATER *2* IN FIGURES 12, 13, AND 14

T	Q	DEC	D-HEAT-EX
P=13sec			
2.07	0.	-0.23936E-01	
1.66	0.	-0.11442E-01	
1.25	0.	-0.69657E-02	
1.25	1.65	-0.94613E-02	0.250E-02
1.25	3.40	-0.11744E-01	0.478E-02
1.25	5.62	-0.15159E-01	0.819E-02
1.25	9.00	-0.20823E-01	0.139E-01
P=26sec			
2.11	0.	-0.39624E-01	
2.11	1.01	-0.40605E-01	0.981E-03
2.11	2.01	-0.42010E-01	0.239E-02
2.11	4.02	-0.43908E-01	0.428E-02
2.11	8.02	-0.49211E-01	0.959E-02
1.50	0.	-0.17481E-01	
1.50	2.00	-0.20217E-01	0.274E-02
1.50	4.04	-0.24255E-01	0.677E-02
1.50	6.04	-0.27887E-01	0.104E-01
1.50	8.03	-0.33569E-01	0.161E-01

Reproduced with permission of the copyright owner. Further reproduction prohibited without permission.

DATA PLOTTED FOR HEATER *2* IN FIGURES 12, 13, AND 14

T	Q	DEC	D-HEAT-EX
	P=38sec		
2.04	0.	-0.39930E-01	
2.04	0.	-0.39489E-01	-0.441E-03
2.04	0.	-0.40306E-01	0.376E-03
1.95	0.	-0.33465E-01	
1.81	0.	-0.26624E-01	
1.62	0.	-0.22887E-01	
1.37	0.	-0.17191E-01	
1.25	0.	-0.16096E-01	
1.25	0.97	-0.17785E-01	0.169E-02
1.25	2.03	-0.20256E-01	0.416E-02
1.25	3.90	-0.27237E-01	0.111E-01
1.25	7.86	-0.42484E-01	0.264E-01

Reproduced with permission of the copyright owner. Further reproduction prohibited without permission.

DATA PLOTTED FOR HEATER *3* IN FIGURES 15, 16, AND 17

T	Q	DEC	D-HEAT-EX
P=13sec			
2.10	0.	-0.54570E-01	
1.82	0.	-0.30075E-01	
1.61	0.	-0.22823E-01	
1.61	0.98	-0.23324E-01	0.501E-03
1.61	2.35	-0.23984E-01	0.116E-02
1.61	4.34	-0.25453E-01	0.263E-02
1.61	6.90	-0.27906E-01	0.508E-02
1.61	10.04	-0.30704E-01	0.788E-02
1.29	0.	-0.17241E-01	
P=26sec			
1.30	0.	-0.25360E-01	
1.30	1.42	-0.28155E-01	0.280E-02
1.30	3.20	-0.31191E-01	0.583E-02
1.30	5.72	-0.39878E-01	0.145E-01
1.30	8.90	-0.44497E-01	0.191E-01
1.30	10.60	-0.50172E-01	0.248E-01
1.61	0.	-0.33154E-01	
1.61	1.51	-0.35722E-01	0.257E-02
1.61	3.37	-0.38464E-01	0.531E-02
1.61	6.04	-0.42002E-01	0.885E-02
1.61	9.51	-0.48241E-01	0.151E-01
1.61	11.43	-0.52519E-01	0.194E-01

Reproduced with permission of the copyright owner. Further reproduction prohibited without permission.

1.89		0.	-0.48514E-01	
2.10		0.	-0.81146E-01	
2.10		1.61	-0.82727E-01	0.158E-02
2.10		3.59	-0.84826E-01	0.368E-02
2.10		6.51	-0.87420E-01	0.627E-02
2.10		10.52	-0.92310E-01	0.112E-01
2.10	P=39sec	0.	-0.94476E-01	
1.87		0.	-0.56483E-01	
1.60		0.	-0.40542E-01	
1.60		2.32	-0.46529E-01	0.599E-02
1.60		4.31	-0.49852E-01	0.931E-02
1.60		7.42	-0.57642E-01	0.171E-01
1.60		9.97	-0.63512E-01	0.230E-01
1.32		0.	-0.33533E-01	

Reproduced with permission of the copyright owner. Further reproduction prohibited without permission.

References

1. L. Landau, J. Phys. U.S.S.R. 5, 71 (1941).
2. L. Tisza, Naure 141, 913 (1938); Compt. rend. 207, 1035, 1186 (1938); J. Phys. et radium, (8) 1, 164, 350 (1940); Phys. Rev. 72, 838 (1947).
3. L. Tisza, Compt. rend. 207, 1035 (1938).
4. V. Peshkov, J. Phys. U.S.S.R. 8, 381 (1944); 10, 389 (1946).
5. H. E. Hall, Proc. Phys. Soc. (London) A67, 485 (1954).
6. D. V. Osborne, Proc. Phys. Soc. (London) 63, 909 (1950).
7. L. Onsager, Nuovo Cimento Suppl. 6, 2249 (1949).
8. An excellent review of work on critical velocities is presented by W. E. Keller, Helium-3 and Helium-4 (Plenum Press, New York, 1969), Chapter 8, p. 273.
9. R. P. Feynman, in Progress in Low Temperature Physies, edited by C. J. Gorter (North Holland Pub. Co., Amsterdam, 1955), Vol. I, p. 17.
10. E. L. Andronikashvili, Zh. Eksperim. i Teor. Fiz. 22, 62 (1950).
11. J. D. Reppy and D. Depatie, Phys. Rev. Letters 12, 187 (1964).
12. J. R. Clow and J. D. Reppy, Phys. Rev. Letters 16, 887 (1966).

Reproduced with permission of the copyright owner. Further reproduction prohibited without permission.

13. R. Penney and A. W. Overhauser, Phys. Rev. 164, 268 (1967).

14. R. J. Donnelly and A. C. Hollis Hallett, Annals of Phys. 3, 320 (1958).

15. K. R. Symon, Mechanics (Addison-Wesley, Reading, Massachusetts, 1961), p. 48.

16. J. D. Reppy, private communication.

17. E. Andronikashvili, J.E.T.P. 18, 429 (1948).

18. A. C. Hollis Hallett, Proc. Roy Soc. (London), A210, 404 (1952).

19. A. de Troyer, A. van Itterbeek, and G. van der Berg, Physica 18, 50 (1951).

20. J. G. Dash and R. D. Taylor, Phys. Rev. 105, 7 (1957).

21. B. Welber and S. L. Quimby, Phys. Rev. 107, 645 (1957).

22. L. D. Landau and E. M. Lifshitz, Fluid Mechanics (Addison-Wesley, Reading, Massachusetts, 1959), p. 93.

23. Landau and Lifshitz, op. cit., p. 51

24. Jahnke and Emde, op. cit., p. 146.

25. Landau and Lifshitz, op. cit., p. 93.

26. T. K. Hunt, Phys. Rev. 170, 245 (1968).

27. These drawn steel wires were purchased from the Secon Metals Corp., White Plains, New York.

28. These small, etched tungsten wires were purchased

Reproduced with permission of the copyright owner. Further reproduction prohibited without permission.

from the Sigmund Cohn Mfg. Co. Inc., Mt. Vernon, New York.

29. E. J. Walker, Rev. Sci. Instr. 30, 834 (1959).

30. H. D. Young, Statistical Treatment of Experimental Data (McGraw Hill, New York 1962), p. 93.

31. G. N. Watson, A Treatise of the Theory of Bessel Functions (Cambridge at the University Press, 1962), PP. 200-201.

32. E. Jahnke and F. Emde, Tables of Functions with Formulae and Curves (Dover, New York, 1945), p. 144.

33. R. J. Donnelly, Experimental Superfluidity (University of Chicago Press, Chicago, 1967).

Reproduced with permission of the copyright owner. Further reproduction prohibited without permission.

Acknowledgements

I would like to express my grateful appreciation to Professor C. T. Lane for his support and advice during the course of my graduate education, to all of the members of the "Low Temperature Group" for their many helpful discussions, and to Dr. John Reppy for his insight at a crucial stage of this work. This experiment was supported by the National Science Foundation and the Army Research Office (Durham).

I would like to thank the staff of the Gibbs and Sloane Machine Shops, especially Stan and Roger, for their able assistance on construction projects, and Grace Gruber for her much appreciated assistance in the preparation of this final document.

Finally, I would like to thank Susy for her support and encouragement during my graduate school career.

Reproduced with permission of the copyright owner. Further reproduction prohibited without permission.